Transient Radicals Produced by Sonication and the Investigation of Paramagnetic Effects

Kacey B. McCreary

Thesis submitted to the faculty of the

Virginia Polytechnic Institute and State University

in partial fulfillment for the requirements for the degree

Master of Science
in
Chemistry

Louis A. Madsen, Chair

Karen J. Brewer

James M. Tanko

September 28, 2012

Blacksburg, Virginia

Keywords: Nuclear Magnetic Resonance, T_1 relaxation, sonication, free radical

Transient Radicals Produced by Sonication

and the Investigation of Paramagnetic Effects

Kacey B. McCreary

Abstract

Ultrasound can be used to create free radicals by growth and collapse of cavitation bubbles. These free radicals have potential use in various fields as seen in the figure below.

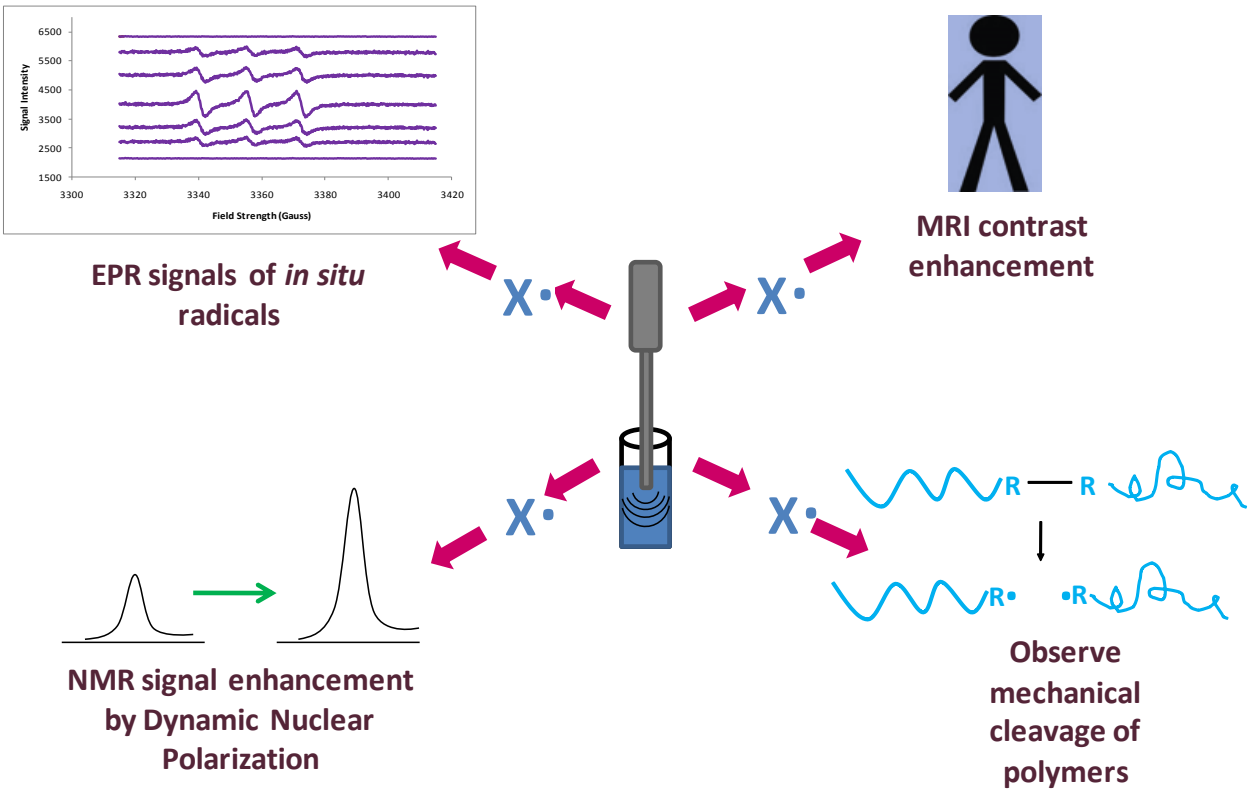

The formation of free radicals can be monitored by decrease in T_1 during NMR experiments due to paramagnetic effects. Our goal is to develop a method in which ultrasound is used to enhance NMR. By irradiating the sample ***during*** analytical measurements, we can decrease T_1 which can be used as a non-toxic contrast agent[1] producing hydroxyl radicals from

the water in the body, invoke NMR enhancement using dynamic nuclear polarization[2], control and understand polymer reactions[3,4], and study the formation of radicals in chemical systems with EPR[5].

The experiments conducted indicated a decrease in T_1 when ultrasound was applied. A maximum decrease was observed when 104 W of ultrasound power was applied and with higher concentrations of radical producing species. Through the experiments it was evident that the sample temperature increased during sonication. To counter this, gated sonication was used to minimize temperature increase. During sonication, the sample was vigorously mixed. Experiments where the sample was mixed through alternate means and theoretical simulations indicate that sample mixing gives an apparent decrease in T_1.

In situ sonication to decrease T_1 shows promise. The question remains if the decrease is due to a combination of radical production and mixing or just an artifact of sample mixing. This is a difficult parameter to determine but future experiments will attempt to supply further conclusions.

Acknowledgements

First, I would like to express my sincerest gratitude to my advisor, Dr. Madsen. He offered unwavering support and critical guidance. Through his passion for research, he ignited my interest and was a tremendous teacher. He was always willing to help and encourage me to learn beyond the obvious. I count him as a mentor and a friend and I appreciate him accepting me into his research group.

I would also like to thank the members of the Madsen research group. Not only did they offer helpful scientific conversations and foster a lab founded on community spirit, they helped make graduate school a fun and memorable experience. I will consider them all life-long friends.

I offer much appreciation to my committee members, Dr. Brewer and Dr. Tanko. They supported me in my journey through offering their support, providing me their knowledge, and guiding me in a way that made me believe in myself.

A special thanks to my close friends who supported me through my graduate career. Without them, graduate school would not have been nearly as much fun and they were a great support group to lean on.

I would also like to thank my parents, my sister, and my family. No matter the trial or personal struggle I was experiencing, they assured me I could do anything I set my mind to. Their love and support means the world to me.

And to my husband, Jonathan, I offer a loving “thank you”. He was there through all the ups and downs and experienced them with me. He cheered me on in my accomplishments and got me ice cream in my failures. He has been my biggest fan and taken every opportunity to tell me.

Finally, I would like to thank God and His son, Jesus Christ. Without the comfort of prayer, I would have never stepped out of my comfort zone.

Table of Contents

List of Figures

Chapter 1
Introduction and Background

1.1 Nuclear Magnetic Resonance

1.1.1 Theory

The experiments conducted for this thesis, discussed in more detail later, involve employing ultrasound to produce free radicals in order to decrease T_1 relaxation. To fully understand this research, it is necessary to start with the fundamentals of Nuclear Magnetic Resonance.

Nuclear Magnetic Resonance (NMR) spectroscopy contains a powerful class of methods used for determining structures and studying dynamics from the molecular to the macroscopic scale. The basis of NMR relies on the intrinsic properties of spin, magnetism, and angular momentum that nuclei exhibit. Nuclei that have a spin quantum number, s, greater than zero will undergo Zeeman splitting when an external magnetic field is applied. The previously equal in energy spin states will lose their degeneracy. When no external magnetic field is applied, the magnetic momentum vectors of the nuclei are random and there is no net magnetic moment. Once the external magnetic field is introduced, each nucleus begins to precess about the magnetic field due to its angular momentum. The frequency of precession, ω°, is the Larmor frequency and Equation 1.1 shows that it is proportional to the magnetic field that the nucleus is experiencing, B°, and the gyromagnetic ratio, γ.[6]

$$\omega^\circ = -\gamma B^\circ \tag{1.1}$$

Because the nuclei are experiencing local fluctuations in the magnetic field, the magnetic moment begins to “wander”, releasing energy through spin flips between the energy states brought on by the Zeeman splitting. After some time, there is a slight bias of spins orienting

parallel to the applied magnetic field than orienting opposed. This slight population difference between spin states gives a net magnetic moment. The difference is given by the Boltzmann population difference in Equation 1.2, where N is the number of spins in the given state, ħ is Planck's constant, γ is the gyromagnetic ratio of the nucleus, B° is the magnetic field strength, k is Boltzmann's constant, and T is temperature.[6]

$$\frac{N_{down}}{N_{up}} = e^{\frac{-\hbar\gamma B^{\circ}}{kT}} \tag{1.2}$$

A radio frequency (RF) pulse is applied perpendicular to the applied magnetic field, which torques the net magnetic moment into the transverse plain. As the net magnetic moment rotates, it gives off a detectable RF signal that decays as the spins return to their original population difference, resulting in a net magnetic moment in the direction of the applied magnetic field. This signal is the free induction decay (FID) in the time domain; Fourier transform gives the characteristic NMR signal in the frequency domain.[7, 6]

1.1.2 T_1 Relaxation

One parameter in the field of NMR is T_1, spin-lattice, relaxation time. As will be discussed later, free radicals decrease T_1 so a fundamental understanding of this parameter and how to measure it, is essential to this project. T_1 is defined as the time it takes for the original Boltzmann population difference to be reached after the RF-pulse is applied. Relaxation back to the original equilibrium state follows an exponential curve, given in Equation 1.3 and shown in Figure 1.1 where T_1 is the time constant of the curve.[6]

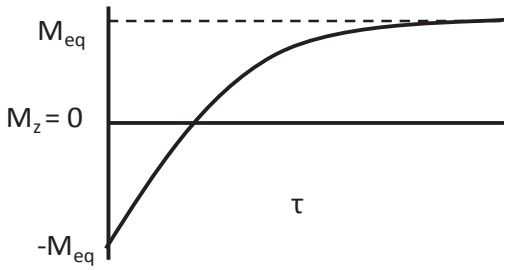

Figure 1.1. Exponential curve of net magnetic moment relaxing back to equilibrium state of original Boltzmann population difference. M_{eq} is the original net magnetization and τ is time.

$$M_z = M_{eq}(1 - 2e^{-\frac{\tau}{T_1}}) \tag{1.3}$$

Another term used for T_1 relaxation is spin-lattice relaxation lending to the idea that the relaxation occurs as the excited nuclei release their excess energy into the surrounding "lattice". A simple way to visualize this process is to picture the precessing nuclei as RF transmitters that release their energy by other precessing species acting as RF receivers. In order for the reception to occur, the two precessing species must have the same frequency. Because the spins are experiencing local fluctuations in the magnetic field, their precession frequency is varying which allows for this energy transfer until equilibrium (original Boltzmann population difference) is reestablished.[6, 8]

A common pulse sequence used to measure T_1 is inversion recovery. The sample is irradiated with a 180° pulse, some time (delay time, τ) is waited, and then a 90° pulse is applied. The 180° pulse torques the net magnetic moment vector into the direction anti-parallel to the applied magnetic field. After the delay, a portion of relaxation has occurred and then a 90° pulse is given to torque the net magnetic moment vector into the detectable plane. The pulse sequence given during the experiment and the corresponding net magnetic moment vector sequence is given in Figure 1.2. The varied delay time is plotted against the maximum signal intensity to give the curve shown in Figure 1.1. Data is fit to Equation 1.3 and T_1 is extracted.[6]

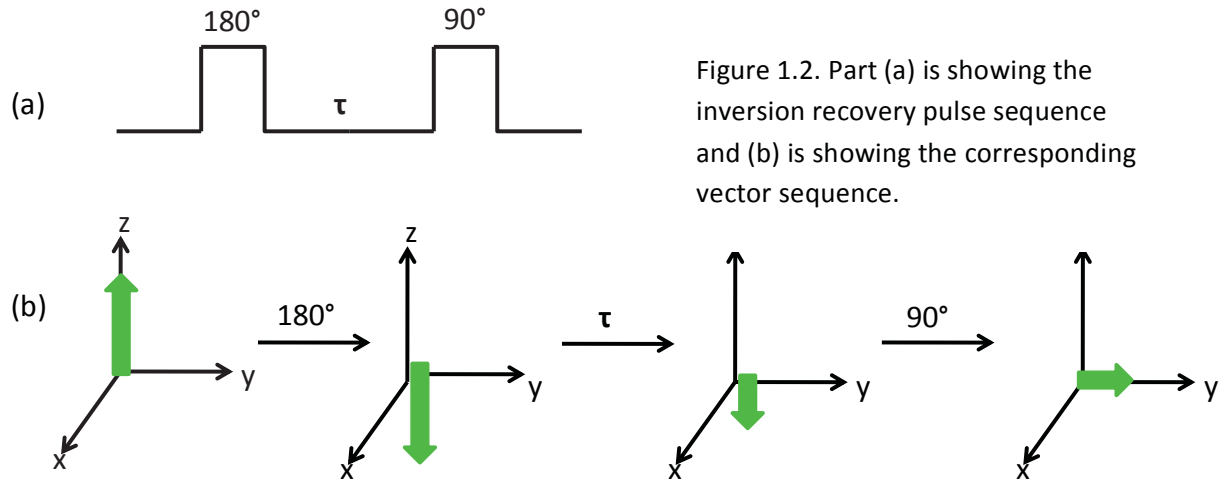

Figure 1.2. Part (a) is showing the inversion recovery pulse sequence and (b) is showing the corresponding vector sequence.

1.2 Sonochemistry

1.2.1 Theory

In the experiments conducted for this thesis, sonication was used a means for radical production. To understand this process, sonochemistry must be defined. Sonochemistry is the study of applying ultrasound to a chemical system and the effects that follow. Introducing chemical system to sounds waves is a useful technique because the interactions occur over a wide range of energies.[9] Ultrasound is in the frequency range of 20kHz to 500MHz which is above the region of human hearing. Sonochemistry specifically involves the power ultrasound region between 20 kHz and 100 kHz. These sound waves are low frequency and high energy.[10]

Ultrasound waves propagate through a liquid sample causing the molecules to oscillate in the same direction of the longitudinal sound wave. As the molecules move with the consecutive waves, areas of compression and rarefaction are produced as is depicted in Figure 1.3.

Figure 1.3. Compression and rarefaction in sound wave. C=compression R=rarefaction

During the compression cycle, molecules are pushed together due to positive pressure. Then during the rarefaction cycle, the molecules are pulled apart due to negative pressure. If the negative pressure exceeds the attractive forces keeping the water molecules intact, a cavitation bubble will form. The amount of negative pressure needed to create a cavitation bubble depends on the liquid and its purity. Mason *et al.* reports a value of 20 atm to create a cavitation bubble which leads to the theory that there must be areas in the liquid that are weakened due to gas molecules and small particles which act as nucleation sites for the cavitation bubbles to form.[10] If a liquid contains an impurity, a gas bubble may be trapped in the fracture of the small particle. During a rarefaction cycle, the trapped bubble will expand and be released into solution leading to a decrease in the tensile strength of the liquid.[9]

If the bubbles are too large, they will simply float to the surface while the smaller ones will dissolve into the liquid. The intermediately sized cavitation bubbles, those with diameters in the micrometer range, will modulate in size due to the positive and negative pressure cycles. Over time, the cavitation bubbles grow, doubling or even tripling in size.[11] The growth of the cavitation bubble is due to the difference in the surface area of the bubble during the cycles. The surface area of the bubble will be slightly larger during the rarefaction cycle and since the amount of gas that will enter the bubble is dependent on the surface area, more gas will enter during rarefaction. This causes the bubble to expand slightly more than it shrinks during each compression and rarefaction cycle. Eventually a maximum radius will be reached where the bubble will expand rapidly in one cycle because it can absorb more energy from the ultrasound. Once this maximum radius is reached during a compression region (high pressure), liquid quickly flows in and the bubbles collapse. A hot spot is created when the cavitation bubbles collapses because the gases inside are compressed. Models have shown the temperature of the hot spot to be in the thousand of degrees Celsius and the pressure the to be on the order of

hundreds to thousands of atmospheres.[1] The process of formation, growth, and collapse is illustrated in Figure 1.4.[11]

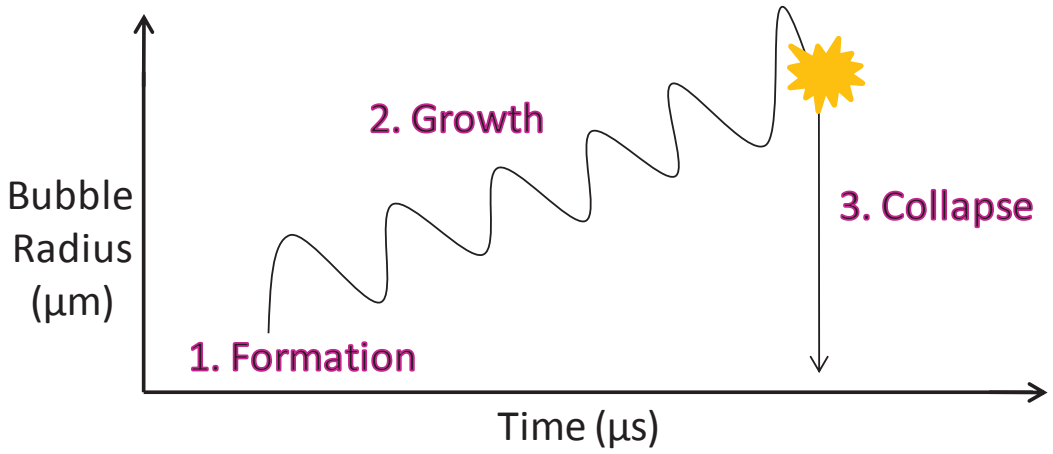

Figure 1.4. The formed cavitation bubble expands and contracts until it eventually collapses.

1.2.2 Radical Formation

Applications in the field of sonochemistry are vast and often based on radical formation; as in the research conducted for this thesis. There are three regions where reactions occur during cavitation due to sonication. An illustration of this can be seen in Figure 1.5. Region one is inside the bubble where extreme pressures and temperatures exist;[11] up to 30,000 K[12] and 1,000 atm.[10] This region can contain either the gas from the sample or volatile components of the sample.[13] In this region of extreme temperature, pyrolysis reactions may occur.[11] Region two is the area around the cavitation bubble separating it from the solvent. In this region reactions can occur due to temperature and pressure gradients. Suslick *et al.*, using a conduction model, reported that the temperatures in this region are around 2000 K in organic liquids. They also estimated that the region occupies an area of about 200 nm from the surface of the collapsing bubble.[14] The third region is the solvent surrounding the bubbles at ambient

conditions. Reactions that occur in regions one and two can form products which react with solute molecules in region three.[11]

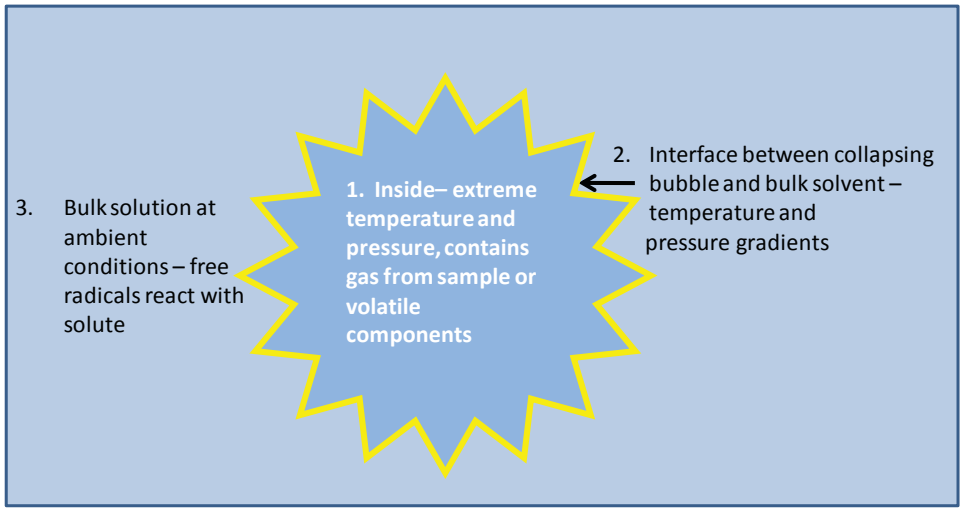

Figure 1.5. The three regions where reactions take place during sonication.

One way radicals can form during sonication is by the extreme heat produced in regions 1 and 2. For example, when aqueous samples are sonicated the bonds of the water molecules are thermally broken in a process called thermal homolysis and two radical species are formed: ·H and ·OH as can be seen in Equation 1.4.[15] These radicals will react with solutes in region 3 of the sample or recombine to form water molecules or hydrogen peroxide (H_2O_2) if there is nothing with which they can react.[16,15,17]

$$H_2O(l) \rightarrow \ {}^{\cdot}H(aq) + \ {}^{\cdot}OH(aq) \qquad (1.4)$$

Radicals can also be formed due to the large pressure gradient in region 2. When a polymer is in solution and a cavitation bubble collapses, the part of the polymer chain nearest the collapsing bubble is more quickly pulled toward the collapsing bubble than the part of the polymer chain farthest from the bubble. In other words, the solvent flow is greatest near the

collapsing bubble and decreases as you move further from the bubble leading to mechanical cleavage (indicating the polymer chain is broken due to the application of a mechanical process – sonication) of the polymer forming two radicals. This can be seen in Figure 1.6.[18]

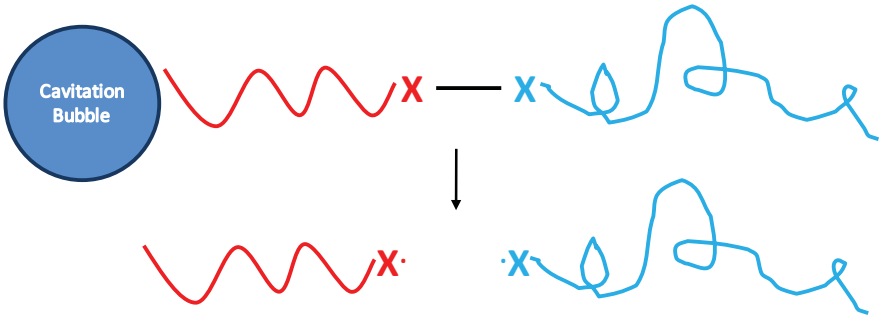

Figure 1.6. Polymer mechanical cleavage due to pressure and flow gradients produced by the collapse of cavitation bubbles.

1.2.3 Parameter Optimization

When performing sonochemical experiments, it is important to understand the parameters that can be optimized to increase the yield of cavitation bubbles and sonochemical products. For our research, this is important to increase radical formation due to the fact that a higher radical concentration will decrease T_1 by a greater amount. These parameters including polarity, volatility, ultrasound frequency and duration, and dissolved gas, are discussed below.

The sonochemically induced decomposition of benzene, 1,4-cyclohexadiene, 1,3-cyclohexadiene, cyclohexene, and cyclohexane in *n*-propanol, *n*-decane, and tetrachlorotheylene were studied by We *et al.* in an attempt to learn about the polarity and volatility effects of solvent and solute. The experiments were conducted by sonicating the system using a titanium ultrasound probe with 24 kHz frequency for 210 minutes. A sample of 0.5 mL was taken at 30 minute intervals and analyzed by GC/MS. Reaction rates were calculated by observing the formation of products. Experiments showed that the polarity of the solute in relation to the polarity of the solvent affects the sonochemical yield by altering the

efficacy by which the solute is transferred to the cavitation bubbles formed in the solvent. Cyclohexane in *n*-decane and benzene in *n*-propane had decreased yields and We *et al*. explained this as the cyclohexane and benzene being unable to go into the cavitation bubbles. Also, the more volatile the solute, the faster the reaction occurred leading to higher sonochemical yields in a given amount of time. The higher the vapor pressure of the solute, the more likely the solute is to transfer to the cavitation bubble.[19]

Riesz *et al*. studied the effects of sonolysis with varied solvents including those with vapor pressures higher than water (methanol[20], ethanol[21], acetone[22], and acetonitrile[22]) and with lower vapor pressure than water (DMSO[23]). In this study, samples were sonicated at 50 kHz and the EPR spectra were taken of spin-adducts formed in the presence of the spin-trap DBNBS (3,5-dibromo-4-nitrosobenzenesulfonate). In the solvents with higher vapor pressure than water, the spin-adduct production decreases at higher concentrations of the solvent. On the other hand, for the DMSO water mixture, the spin-adduct increases with increased concentration of DMSO.[24] Perhaps the solvents with higher vapor pressure are too volatile and too much of the solvent vapor is getting into the cavitation bubble instead of the solute.

Optimizing ultrasound frequency significantly impacts sonochemical experiments. When water is sonicated hydroxyl radicals are formed which can then recombine to form hydrogen peroxide.[25] Monitoring the hydrogen peroxide formation rate can be an indicator of sonochemical efficiency by monitoring the concentration of hydrogen peroxide formed versus sonication frequency. One experiment was conducted at a frequency of 514kHz and 20kHz under both oxygen and argon. Under both gas conditions, the rate of hydrogen production was higher when the 514kHz ultrasound was used. At higher ultrasound frequencies the cavitation bubbles produce less heat and have a shorter lifetime. Since the recombination of hydroxyl radicals to form hydrogen peroxide happens outside of the bubble region, more hydroxyl radicals form with the conditions occurring at higher frequencies. With higher frequencies, more

radicals are produced (due to shorter lifetimes of bubbles) and more radicals make it to the region outside of the bubble (the lower temperature leads to less reactions occurring inside the bubble).[25]

Another experiment was conducted by Okitsu *et al.* in which the effects of ultrasound frequency were studied pertaining to the synthesis of gold nanoparticles in the presence of 1-propanol. In order for the nanoparticles to form, the gold must be reduced which is possible due to the free radicals produced during sonication. The more radicals produced, the faster the rate of reduction. Figure 1.7 shows that for this system an optimum frequency is achieved at 15 kHz.

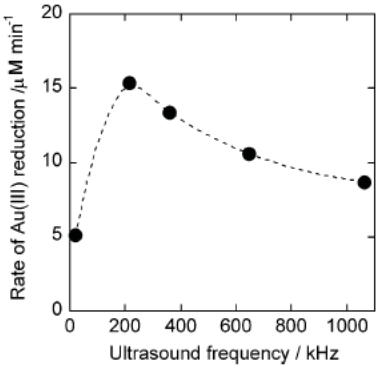

Figure 1.7. This image was copied from Reference 22 and shows that sonochemical yield reaches a maximum at a certain frequency and then declines.

Higher frequencies lead to a decrease in reduction rate. This is explained by the fact that there is a correlation between frequency and cavitation bubble collapse time. At higher frequencies the bubbles collapse faster and the solute molecules spend less time in contact with the collapsing bubbles. Once the frequency reaches an optimal level, there is a reduction in radicals produced at higher frequencies.[26]

Sonication time also affects the outcome of sonochemically induced reactions. Figure 1.8 shows data representing this.

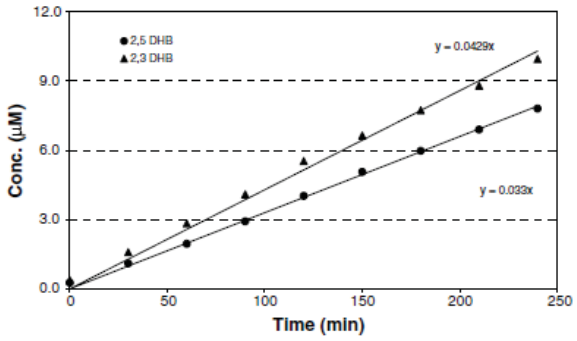

Figure 1.8. Data showing that radical yield linearly increases as sonication time increases. Figure was copied from reference 27.

The data collected for Figure 1.8 was conducted by measuring the concentration of 2,5-dihydroxybenzoic acid and 2,3-dihydroxybenzoic acid which are the major products of the oxidation of salicylic acid. The aqueous system was sonicated and the hydroxyl radicals reduced salicylic acid; therefore, by measuring the concentration of the two products, the effectiveness of the sonication can be observed, where a higher concentration of the products indicates more effective sonication.[27]

One experiment has also shown that the type of gas dissolved in the system being studied plays a role in the enhancement of the sonochemical yield. The gas molecules in a solution can be used as nucleation sites for the cavitation bubbles to form therefore the amount of gas as well as the type of gas, affects the cavitation. Very soluble gasses can decrease cavitation because the quantity of gas bubbles is so large that the cavitation bubbles dissolve into them. Atomicity is another issue to consider. For example, monatomic gasses have a higher heat capacity than diatomic gasses and therefore produce more heat during cavitation bubble collapse.[13] Figure 1.9 shows selected properties of different gasses used in the sonochemically induced dissociation of carbon disulfide. The reaction was monitored by absorbance at 379 nm, where the highest absorbance is indicative of the most efficient sonochemical environment. The dissociation rate decreases as a function of the studied dissolved gasses in the following order He>H_2>air>Ar>O_2>CO_2.[28]

Gas	TC	γ	$S(X_\sigma/10^{-4})$	Abs.
Air	58.3	1.39	-	0.25±0.001
Ar	40.1	1.67	4.9	0.20±0.05
H_2	417.4	1.40	1.6	0.297±0.0005
He	343.4	1.67	1.2	0.31±0.02
O_2	59.4	1.39	4.4	0.17±0.02
CO_2	35.6	1.29	32.8	0
CS_2	16.5	1.22	-	-

Figure 1.9. This image was adapted from Reference 28. TC is the thermal conductivity, γ is the heat capacity ratio at 25°C, S is the solubility at 25°C, and Abs is the measured absorbance at 379.

In summary of the literature, the polarity relationship between solvent and solute will be vital in that we should choose systems that have solutes that will effectively go into the cavitation bubbles. Also the more volatile a solute, the higher the sonochemical yield. It is equally important to test varied frequencies to find an optimal value that leads to a higher concentration of free radicals. Sonication should last for the longest time period possible in a given experiment to increase radical production. Another aspect to consider is the type of dissolved gasses in these experiments because monoatomic gasses have been shown to produce more heat during collapse and consequently, more radicals.

1.3 Research Goals

The goal of our research is to employ sonication for the formation of transient radicals in order to decrease T_1. Free radicals are paramagnetic species defined as containing one or more unpaired electrons. In aqueous samples, the unpaired electrons have a dipolar interaction with water molecules nearby.[29] Dipolar interactions occur in the several angstrom range where the dipolar interaction decreases as $1/r^3$ where r is the distance between nuclei. The interaction

causes the spin angular momentum vectors to flip allowing them to release their energy into their surroundings and return to the original Boltzmann population difference. Unpaired electrons have a 700 times larger magnetic moment than the hydrogens in the sample. Because of the large magnetic moment of the electrons, the hydrogens have a greater dipolar interaction with them, resulting in a shorter T_1.

Several factors are involved in the extent to which T_1 is decreased due to the introduction of a paramagnetic species. Equation 1.5 identifies these factors where μ is the effective magnetic moment, ε is the solvent viscosity, k is the Boltzmann constant, T is absolute temperature, γ is the gyromagnetic ratio, and N is the number of ions per unit volume (concentration). It can be seen that a decrease in T_1 is directly proportional to the concentration of the paramagnetic species.[30]

$$\Delta\frac{1}{T_1} = \frac{12\pi^2\gamma^2\varepsilon\mu^2 N}{5kT} \tag{1.5}$$

The concept of decreasing T_1 by introducing a paramagnetic species is used in contrast agents for Magnetic Resonance Imaging, or MRI. Contrast agents are used to increase the light and dark contrast in an image as seen in Figure 1.10.[31] This is done by introducing paramagnetic species into the body. These paramagnetic species are absorbed into different parts of the body at different rates and amounts, causing a decrease in T_1 of water in those areas which gives a greater contrast.

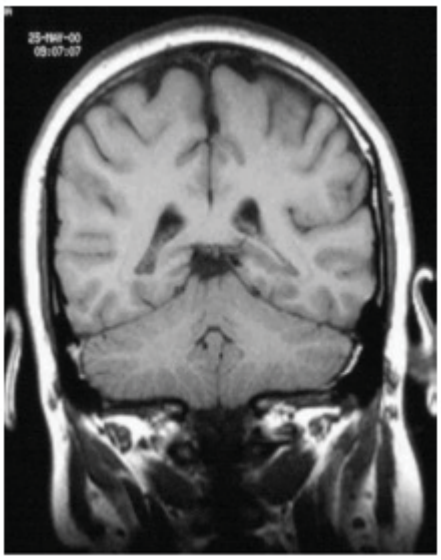

Figure 1.10. This figure was copied from Reference 31 and shows an MRI image of a human brain.

Many commercially available contrast agents contain chelated gadolinium as the paramagnetic species; one example is Omniscan™. Figure 1.11 shows that with higher concentration of the paramagnetic species, Omniscan™ in this case, T_1 is more effectively decreased. The data is reported in terms of relaxivity which is equal to the inverse of T_1.[32]

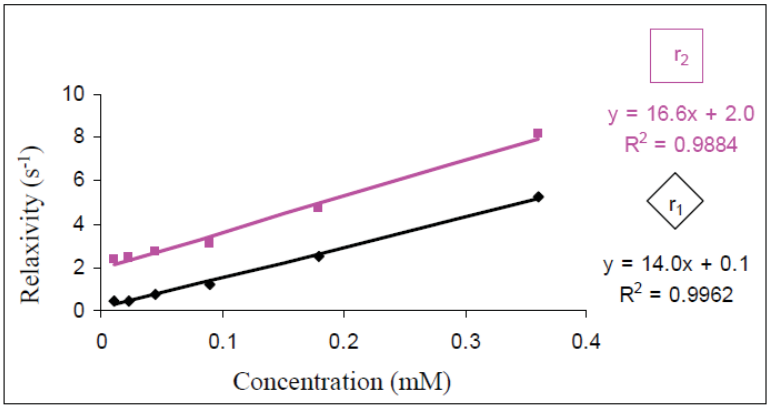

Figure 1.11. This image was copied from Reference 32. This figure shows that as concentration increases, paramagnetic effects increase.

Why does increased concentration increase relaxivity (decrease T_1)? The number of water molecules per paramagnetic gadolinium atoms in a 0.3600 mM solution is 1.5×10^5 and it is 5.1×10^6 for a 0.0110 mM solution.[32] Since the increase in relaxivity is due to the dipolar

interaction between the gadolinium atoms and the hydrogens, in higher concentrations each gadolinium has to interact with fewer water molecules. Another way to think about this is that in higher concentrations, there are more gadolinium atoms to interact with the same amount of water molecules.

Given the concentrations of $GdCl_3$, the sphere of water molecules per gadolinium ion can be calculated. For the 0.3600 mM concentration the sphere has a radius of 10.3 nm and for the 0.0110 mM the radius is 33.0 nm. The relaxivity of the 0.3600 mM is 5.2605 s^{-1} and for the 0.0110 mM it is 0.4332 s^{-1}.[32]

The diffusion of water molecules is also important to think about when considering concentration effects and can be calculated by the Stokes Einstein Relation, Equation 1.6. In the equation *k* is the Boltzmann constant, *T* is temperature, η is viscosity, and *r* is the radius.[33] The diffusion of water at 20°C is 2.295x10^{-9} m^2/sec.

$$D = \frac{kT}{4\pi\eta r} \tag{1.6}$$

$$r_{RMS} = \sqrt{2D\Delta} \tag{1.7}$$

$$\omega° = -\gamma B° \tag{1.8}$$

The average distance travelled, r_{RMS}, can be calculated by Equation 1.7 where Δ is the diffusion time. To determine how far the water molecule diffuses in one Larmor Precession, the diffusion time used in Equation 1.7 is the time it takes for one Larmor Precession which can be found using Equation 1.8. In Equation 1.8, ω° is the Larmor Frequency, γ is the gyromagnetic ratio, and B° is the field strength of the NMR magnet. In this calculation a field strength of 0.36 T is used because that is the field strength of the magnet used in the research that follows.[6, 34] The time for one Larmor Precession is found to be 6.67x10^{-8} sec and the average diffusion distance during that time is calculated at 17.5 nm.

For the lower concentration of $GdCl_3$, the radius of the water sphere is larger than the diffusion length while for the higher concentration, the diffusion length is larger. Because the water molecules need to be close to the gadolinium for the hydrogens to be affected (which increases relaxivity), some of the water molecules in the lower concentration will not diffuse far enough to be affected. This results in fewer hydrogens in the water molecules to participate in dipolar interactions with the paramagnetic gadolinium and the relaxivity is increased less.

In Figure 1.11, it can be seen that a concentration of 0.2 mmol of Omniscan™, which contains a paramagnetic gadolinium, causes a decrease in T_1 by a factor of two. At this concentration, there are approximately 3×10^5 water molecules per gadolinium. This is a substantial decrease in T_1 with only a small concentration of paramagnetic gadoliniums. Using this as an estimate for our research, it can be determined that in order to see a decrease in T_1, the concentration of radicals that needs to be produced is very minimal.

In the literature discussed above (section 1.2.3), the monitoring of free radical production was conducted either by tracking products of reactions occurring because of free radicals or by EPR of trapped free radicals. Previous investigations have either examined a sample after sonication or used a spin-trap to form a stable radical for EPR detection.[35] [23] [16] Our goal is to produce radicals within an NMR. **By using a small, tabletop NMR, the sample can be sonicated while simultaneously experimentally measuring T_1 as means to investigate the possible formation of free radicals.**

Applications for transient radicals in magnetic resonance include use for Dynamic Nuclear Polarization (DNP), medical MRI contrast agents, and understanding reactions involving polymers. DNP can be used to enhance NMR signals by adding paramagnetic species and irradiating with microwaves at the electron's Larmor Frequency.[36] Some contrast agents contain toxic elements that need to be chelated so they are released from the body.[29] By sonicating certain parts of the body as opposed to administering contrast agents, the toxicity

issue might be resolved in some cases. Sonication during reactions could be used in polymer synthesis as free radicals are frequently used in polymerizations.[18 4]

Furthermore, the sensitivity and resolution of NMR is often limited by sample concentration (number of spins) and the strength of the magnetic field. Use of ultrasound-generated transient radicals might help improve sensitivity because the radicals would decrease T_1. Because experimental time is dependent on T_1, a decrease would allow for more scans per unit time.

In our experiments, a tabletop TeachSpin NMR was used to measure T_1 values **while** sonicating the sample. The details of the instruments used are discussed in chapter 2 of this document. By monitoring T_1 effects during sonication, we will gain insight into how ultrasound produces sonication as well as how the paramagnetic species affect the relaxation of the nuclear spins.

Chapter 2
Experimental Methods and Data

2.1 Instrumentation

In order to investigate the effects of sonication on T_1, and thus probe *in situ* radical formation for potential NMR experimental enhancement using ultrasound, a tabletop NMR and probe ultrasound generator were used for *in situ* measurements. The instruments are detailed in the sections below.

2.1.1 TeachSpin

A TeachSpin PS1-A pulsed NMR spectrometer was used for measuring relaxation time constants. This instrument is an ideal choice as it is easily set-up to understand the parameters of NMR spectroscopy due to its "teaching" design. Also, with this instrument, *in situ* measurements were easily obtained because the sonication probe fit directly into the sample within the magnet. Figure 2.1 shows the permanent magnet and the spectrometer which is connected to a Tektronix oscilloscope. The oscilloscope is used to read signal intensities, pulse widths, and FID signals.[34]

(a) 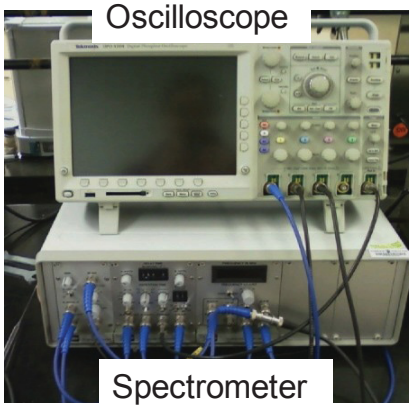

(b) 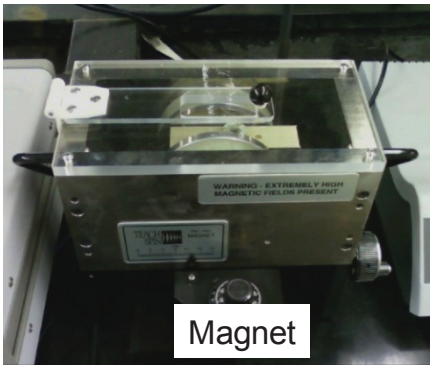

Figure 2.1. The photos are (a) the Teachspin NMR spectrometer interfaced with an oscilloscope and (b) the permanent magnet.

A block diagram of the instrument is presented in Figure 2.2. The pulse programmer is responsible for producing the pulse stream to the oscillator and triggering the oscilloscope. The RF synthesized oscillator generates RF pulse bursts which are amplified by the RF amplifier and sent to the transmitter coils in the sample probe. These RF pulses can be varied in width (duration), spacing, number, and repetition time.[34]

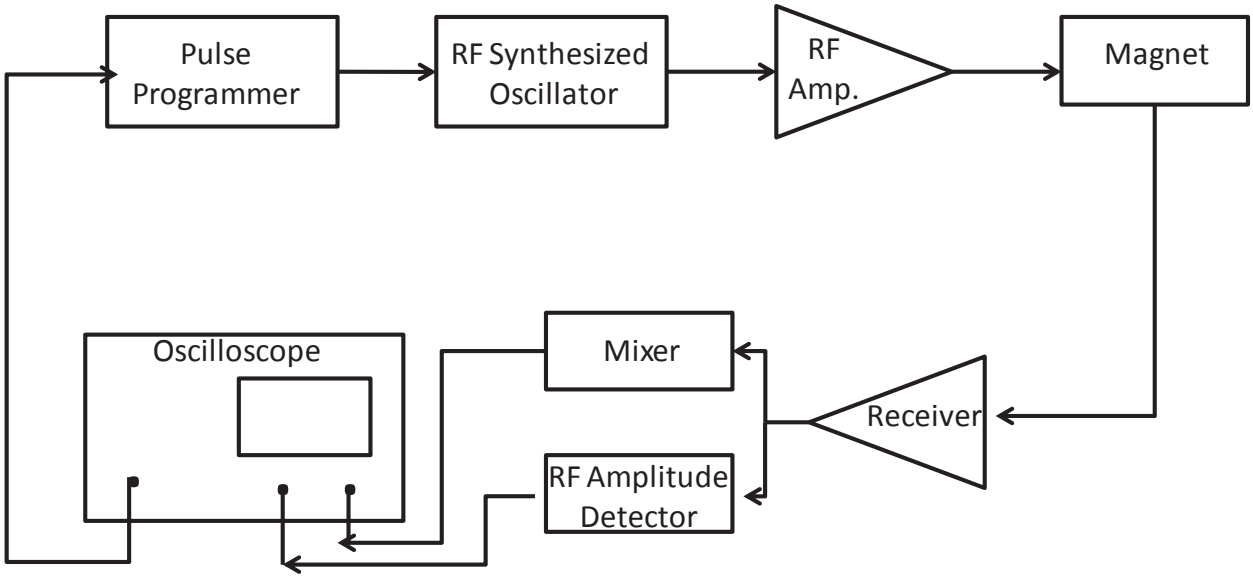

Figure 2.2. Block diagram of TeachSpin NMR.

The transmitter coils are in a Helmholz configuration and produce a 12 gauss rotating magnetic field at the sample in order to create RF pulses that torque the net magnetic moment of the nuclear spins in the sample. The rotating nuclear magnetization in the transverse plane creates a detectable RF signal that is picked up by the receiver coil. The receiver coil is in a solenoid configuration wrapped around the sample vial. Figure 2.3 shows a diagram of the magnet showing the separate, orthogonal transmitter and receiver coils.[34]

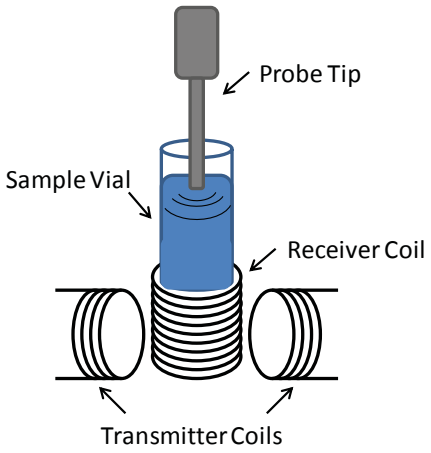

Figure 2.3 Illustration showing orthogonal NMR receiver and transmitter coils, and sample and ultrasound probe.

The RF signal is amplified in the receiver and sent to two different detectors. The RF amplitude detector gives a signal on the oscilloscope proportional to the peak amplitude of the FID. This is the signal used to obtain experimental data. The second detector is a mixer which is used to determine the correct frequency for the synthesized oscillator. The signal from the mixer is proportional to the difference between the RF signal from the precessing magnetization of the sample and the synthesized oscillator. An output of zero from the mixer signifies that the oscillator is tuned to the frequency of the sample.[34]

The magnet used with the TeachSpin NMR is a permanent magnet. The field strength of the magnet is 0.36 T and protons precess in this field at 15.3 MHz. Once the sample is placed within the magnet, it can be moved horizontally and vertically to find an area where the homogeneity of the magnetic field is at a maximum.[34]

2.1.2 Ultrasound

By inserting the probe into the sample (Figure 2.4), direct sonication can be performed. Indirect sonication is used for ultrasonic cleaning baths. The sound waves in indirect sonication pass through some medium before interacting with the sample container of the reaction mixture.[13] For our experiments, it is imperative to employ direct sonication to produce cavitation-induced free radical species.

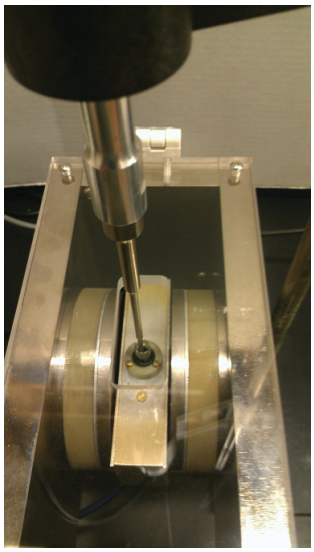

Figure 2.4. Photo of *in situ* sonication. The sonication probe is directly sonicating sample in magnet of Teachspin NMR.

The samples in this research were sonicated using a VCX-130 microprocessor – controlled ultrasound generator (Sonics and Materials Inc., Newtown, CT) for small volume samples. The instrument is shown in Figure 2.5a. This ultrasound generator works by converting voltage to high frequency electrical energy (20 kHz). The electrical energy is then converted to mechanical vibrations by means of a piezoelectric transducer.[37] A piezoelectric transducer is an electrochemical transducer and is made of a piezoelectric material that will expand and contract in the presence of an alternating electric field producing sound waves.[13]

The vibrations are amplified by the titanium alloy probe, which produces ultrasound waves. The probes used in the following experiments were stepped microtips, making them easily fitted into small samples. The probes used were 2 mm and 3 mm in diameter. The 2 mm probe is capable of sonicating samples of 150 µL to 5 mL and the 3 mm probe can sonicate samples of 250 µL to 10 mL. The larger probe can process a larger volume of sample but sacrifices ultrasound wave intensity.[37] These probes can be seen in Figure 2.5b.

(a) 

(b) 

Figure 2.5. The VCX-130 microprocessor- controlled amplifier is shown in (a) and the two microtips, 2 mm and 3 mm, are shown in (b).

The VCX-130 has a maximum power of 130 watts. This can be adjusted by changing the percent amplitude, which changes the power supplied to the ultrasound generator. The frequency of the sound waves produced is 20 kHz.[37]

2.2 Varying Experimental Parameters

In the following experiments, the T_1 of each sample was measured in the TeachSpin NMR without ultrasound application by the VCX-130 generator and then with ultrasound so that the decrease in T_1 could be calculated.

To measure T_1, the sample was placed into the magnet and the instrument was tuned to resonance. The sample was then moved within the magnet to find the area of maximum field strength homogeneity. Accurate pulse widths for the 90° and 180° were obtained by finding the maximum and minimum signal respectively. The spectrometer was set-up to give the 180° pulse, wait some delay time, and then give the 90° pulse. The delay time was varied and the maximum amplitude was recorded for each. A plot, like the one in Figure 1.1, was constructed in Excel™. The solver function was used to find T_1 of the sample. Figure 2.6 shows and

example of raw data taken from NMR measurements and the fit used to extract T_1 using Excel™. The decreases in T_1 are reported at $T_1/T_{1(0)}$, where T_1 is the observed T_1 during sonication (or bubbling) and $T_{1(0)}$ is the T_1 of the sample with no influence.

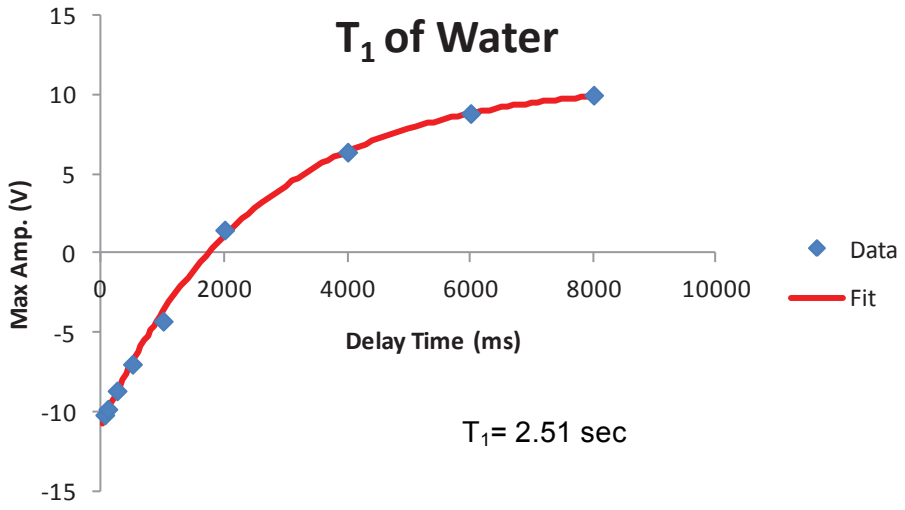

Figure 2.6. Example of inversion recovery Plot of data and fit to extract T_1 using Excel™. This example is presented as one experimental trial

2.2.1 Concentration Dependence

As discussed in section 1.3 of this document, the concentration of the paramagnetic species is directly proportional to T_1. In order to maximize the decrease in T_1, the concentration of the species that would form paramagnetic free radicals was varied. This experiment would show if, in fact, the concentration of the free radical producing species is a factor in the decrease of T_1.

When hydrogen peroxide is sonicated it decomposes by thermal homolysis into two hydroxyl radicals. One set of experiments was conducted in which the concentration of hydrogen peroxide was varied and the decrease in T_1 was observed. The hydrogen peroxide samples were prepared by diluting commercially available un-inhibited 30% hydrogen peroxide with deionized water. Figure 2.7 shows the results. From this plot it can be seen that as the

concentration of hydrogen peroxide was increased, and with ultrasound power of 104 watts, T_1 decreased by a larger amount. Comparing 10% hydrogen peroxide to 30% hydrogen peroxide, T_1 decreased by 11% more with the 30%. It should also be noted that the amount of energy needed to break the oxygen-oxygen bond in hydrogen peroxide is lower than that necessary to break the oxygen-hydrogen bond in water, which is the solvent. The bond enthalpy of the oxygen-hydrogen bond is 464 kJ/mol while the bond enthalpy for the oxygen-oxygen bond is 138 kJ/mol.[38] Since water also forms hydroxyl radicals when sonicated, this fact shows that the concentration of aqueous hydrogen peroxide solutions, as opposed to just water, can be investigated as it takes less energy to form the hydroxyl radicals produced in hydrogen peroxide.

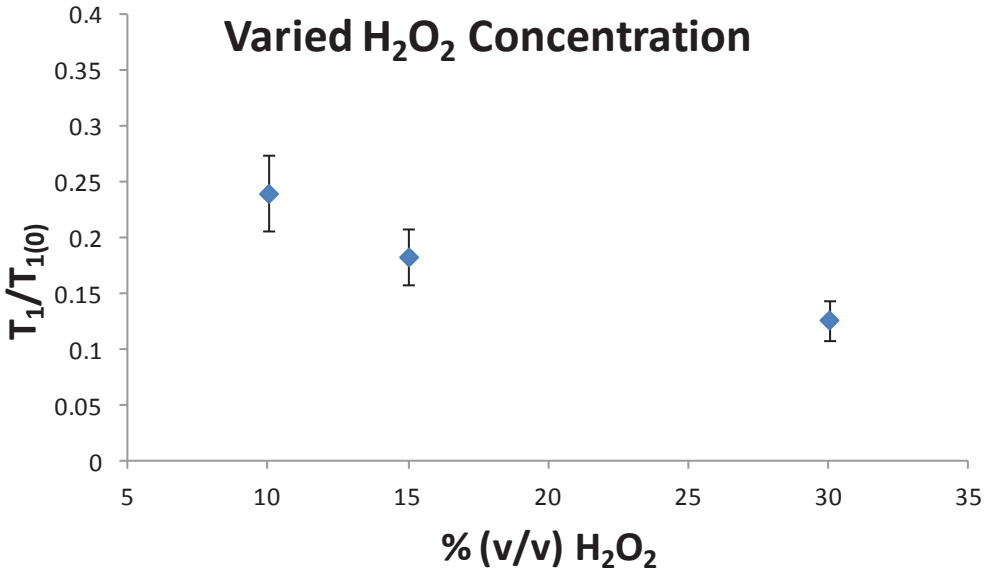

Figure 2.7. Varied concentration of hydrogen peroxide and the effect on T_1. Decrease shown as $T_1/T_{1(0)}$, where T_1 is the measured T_1 during sonication and $T_{1(0)}$ is the T_1 measured when sample is not sonicated. Data presented from one experimental trial with estimated error. $T_{1(0)}$ is 1.45 s, 1.50 s, 1.73, for 10%, 15%, 30% respectively.

With the help of Ms. Rachel Leslie, the data in Figure 2.8 was collected. This data shows that increasing the concentration of benzoyl peroxide, shown in Equation 2.1, does increase the

paramagnetic effect on T_1. The concentrations of benzoyl peroxide/copper sulfate in the three concentration ratios represented on the graph are 0.017 M/0.015 M, 0.024 M/0.020 M, and 0.082 M/0/005 M.

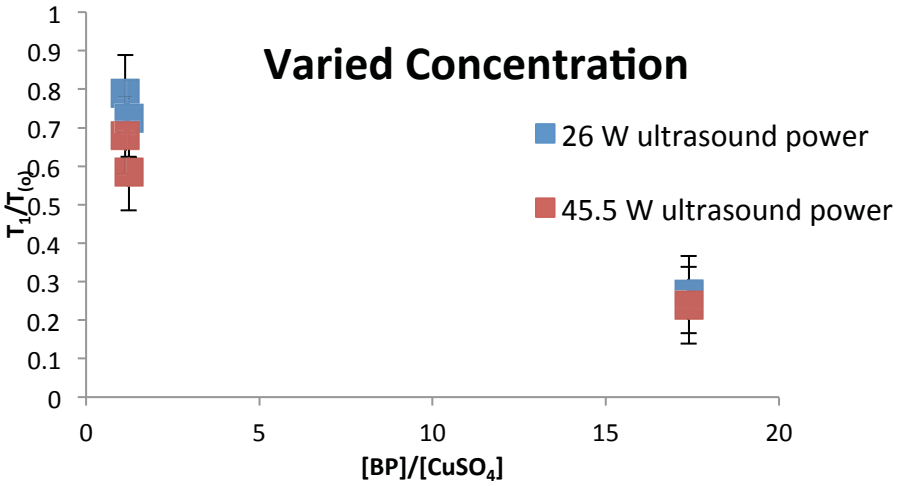

Figure 2.8. Varied concentration of benzoyl peroxide (BP) and copper sulfate, $CuSO_4$, and the effect on T_1. Decrease shown as $T_1/T_{1(0)}$, where T_1 is the measured T_1 during sonication and $T_{1(0)}$ is the T_1 measured when sample is not sonicated. Data presented from one experimental trial with estimated error. $T_{1(0)}$ values are 117 ms, 119 ms, 373 ms corresponding to [BP]/[$CuSO_4$] of 1.13, 1.23, and 17.4 respectively.

In this set of experiments the concentrations of copper sulfate and benzoyl peroxide were varied. The copper in copper sulfate is paramagnetic so it will decrease T_1. Benzoyl peroxide will form free radicals upon sonication due to thermal hemolysis and can be seen in Equation 2.1.

(2.1)

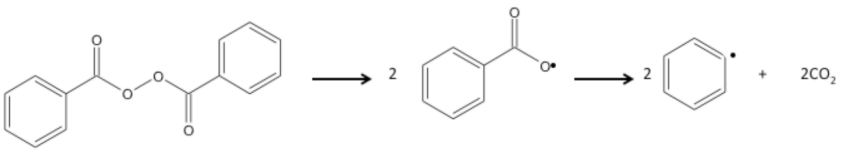

2.2.2 Sonication Amplitude Dependence

In section 1.3 of this document, literature was presented showing the effects of ultrasound frequency on free radical production. The data supported the fact that more radicals are produced at higher frequencies but at some maximum, the production of free radicals decreases.[25, 26] The VCX-130 ultrasound generator sonicates at a frequency of 20 kHz which cannot be adjusted. The amount of power supplied, however, can be adjusted as a function of percent amplitude. A percent amplitude of 100% corresponds to 130 watts of power being supplied. Experiments were conducted to see if the amount of power, percent amplitude, supplied during sonication affected the T_1 decrease, corresponding to a higher yield of free radicals. The range used was kept between 26 W and 104 W ultrasound power per accuracy considerations given in the manual.[37]

Figure 2.9 shows that when sonicating 30% uninhibited hydrogen peroxide, there is a slight increase in the amount by which T_1 is decreased when sonicating with 30 W power as compared to 130 W power. Also, the microtip size was varied used (2 mm and 3 mm) and it can be seen from the graph that there was not a significant difference in their decreasing effect on T_1 ($T_1/T_{1(0)}$= 0.08 using the 3 mm probe compared to 0.13 using the 2mm probe). This is expected as the sample volume is so small.

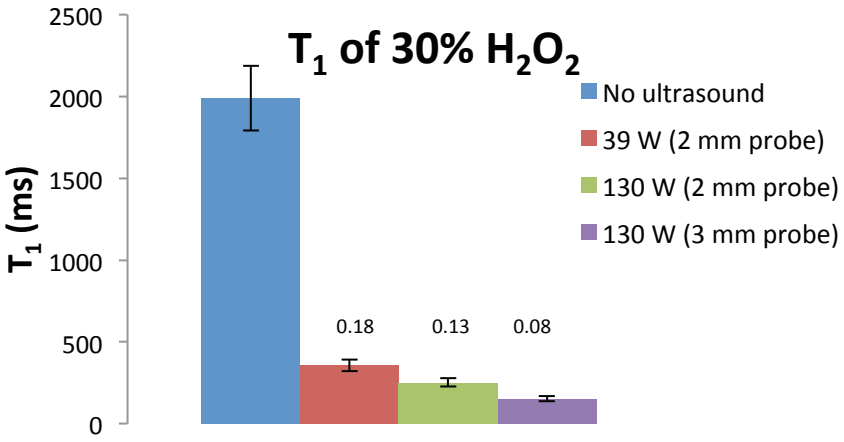

Figure 2.9. T_1 dependence on ultrasound power for 30% H_2O_2 in H_2O. Values above bar indicate decrease in T_1 shown as $T_1/T_{1(0)}$, where T_1 is the measured T_1 during sonication and $T_{1(0)}$ is the T_1 measured when sample is not sonicated. Data presented from one experimental trial with estimated error.

Varied ultrasound power experiments were also performed on deionized water and the results are plotted in Figure 2.10. Again, there is a greater decrease in T_1 when higher power of ultrasound is used. It can be seen in this set of experiments, too, using the 2 mm probe verses the 3 mm probe shows no considerable difference.

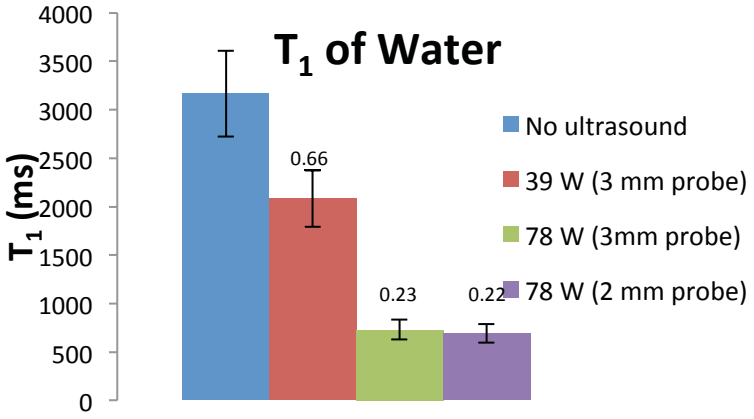

Figure 2.10. T_1 dependence on ultrasound power for deionized water. Values above bar indicate decrease in T_1 shown as $T_1/T_{1(0)}$, where T_1 is the measured T_1 during sonication and $T_{1(0)}$ is the T_1 measured when sample is not sonicated. Data presented from one experimental trial with estimated error.

When comparing the trends seen in the ultrasound power effects on deionized water and the effects on hydrogen peroxide, a difference should be noted in the two sets of data. Figure 2.11 shows both sets of data.

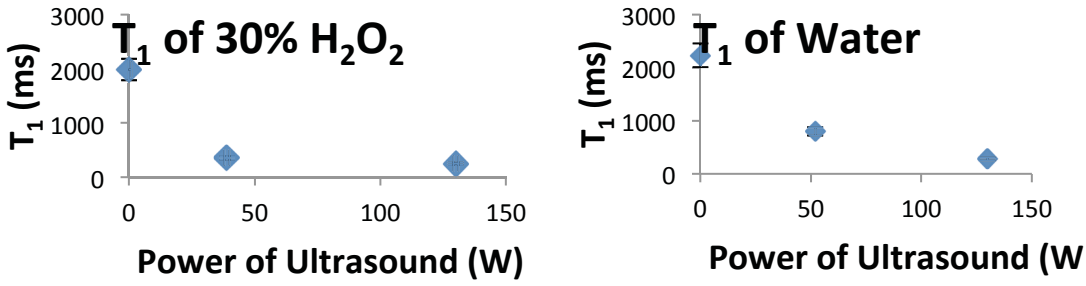

Figure 2.11. Relationship between T_1 and ultrasound power.

Looking at the two plots in Figure 2.11, it can be seen that the decrease of T_1 of deionized water as a function of ultrasound power has a more gradual decrease than that of 30% hydrogen peroxide. The trend in the case of the 30% hydrogen peroxide seems to be leveling off. This may be related to the bond enthalpies in that the oxygen-oxygen bond takes less energy to break than the oxygen-hydrogen bond. Also, when one molecule of hydrogen peroxide is cleaved, two hydroxyl radicals are produced which can interact with the neighboring hydrogens. Since concentration of the paramagnetic species is a factor in the decrease in T_1, it would make sense that when more free radicals are produced, a larger decrease is observed. In this case it corresponds to the decrease happening with less ultrasonic power supplied to the system.

Another set of data, seen in Figure 2.12, shows the correlation between ultrasound power and T_1 decrease. The same trend as discussed before is seen here but this data also shows that the power supplied is most accurate in the 26 W to 104 W region because the data show a more linear relationship.

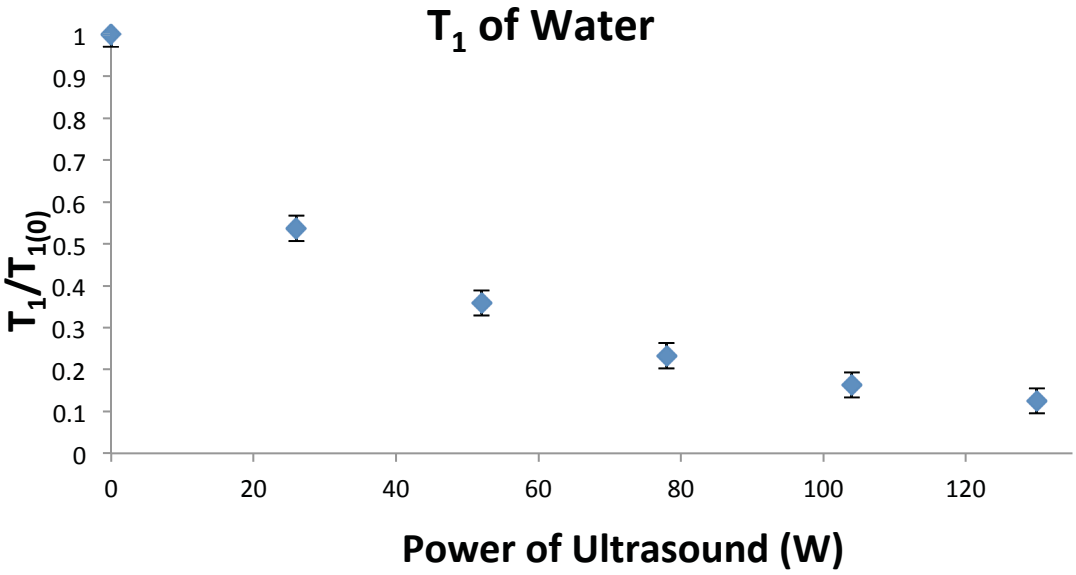

Figure 2.12. Relationship between T_1 of deionized water and ultrasound amplitude. Decrease shown as $T_1/T_{1(0)}$, where T_1 is the measured T_1 during sonication and $T_{1(0)}$ is the T_1 measured when sample is not sonicated.

It should be noted that the data collected for Figure 2.12 is an average over 2 trials. The separate trials are plotted in Figure 2.13.

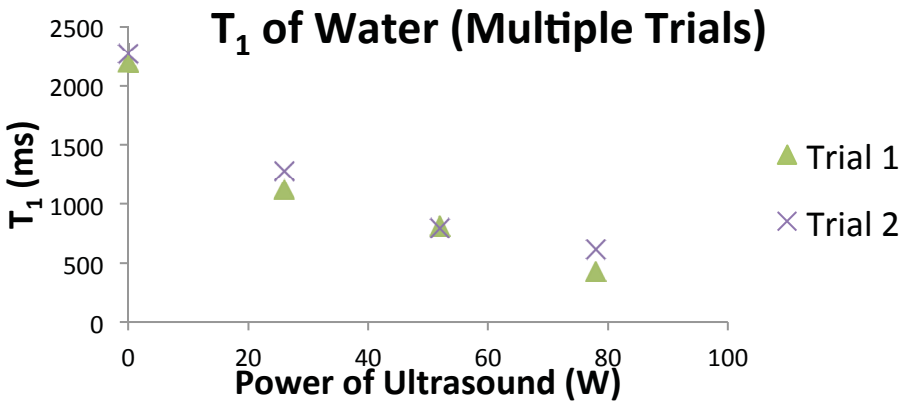

Figure 2.13. Multiple trials of raw data of deionized water sonicated at varied ultrasound powers.

2.2.3 Summary

To summarize the results of section 2.2 of this document, concentration of free radical producing species and the power (percent amplitude of ultrasound) were varied as the decrease in T_1 was monitored. Experiments were conducted in which the concentration of hydrogen peroxide and benzoyl peroxide were increased leading to a larger decrease in T_1 upon sonication. In both hydrogen peroxide and benzoyl peroxide, the oxygen-oxygen bond is expected to break to form transient free radicals.

By varying the percent amplitude of sonication, the power supplied to the ultrasound generator was changed. The amplitude is related to how far the probe moves away from its equilibrium point during sonication where an increase in percent amplitude indicates that this distance is increased. The data showed that in both deionized and hydrogen peroxide systems, an increase in power leads to a greater decrease in T_1. The trend observed for the deionized water at a more gradual decrease in T_1 has more ultrasound power was supplied to the sample. This is believed to be due to the difference in energy requirements for breaking bonds in order to form free radicals; less energy is needed to break the oxygen-oxygen bond than the oxygen-hydrogen bond.

2.3 Pulsed Sonication

In the experiments presented in section 2.2 of this document, the sample was subjected to ultrasound during the entire experiment which lasted 15 to 20 minutes. Literature reports that the heat produced from the collapsing cavitation bubbles disperses so quickly that the bulk temperature of the solution is not affected. The rate of cooling is estimated to be over 1,000,000,000 °C/s.[9] Figure 2.14 shows experimental evidence that the temperature of the sample (deionized water in this case) does increase to some extent during sonication over the period of measuring T_1 with the temperature increase being correlated to the power of ultrasound applied. At each ultrasound power, the T_1 was obtained via inversion recovery. At

the end of the experiment, which took 20 ± 2 minutes, a thermocouple attached to a multimeter was directly inserted into the sample vial to measure the temperature. While the sample was likely to be cooled slightly because it took some time (estimated at 5 seconds) to insert the thermocouple and the thermocouple was at room temperature, an obvious trend in temperature increase is still apparent. When a deionized water sample is heated to 31.1°C after 10 seconds of 40% ultrasound amplitude, it takes 5 minutes for the sample to return to the original room temperature of 25.9°C. Based on that observation, it can be estimated that in the 5 seconds to insert the thermocouple into the sample, the temperature has only decreased 0.1°C which is minimal.

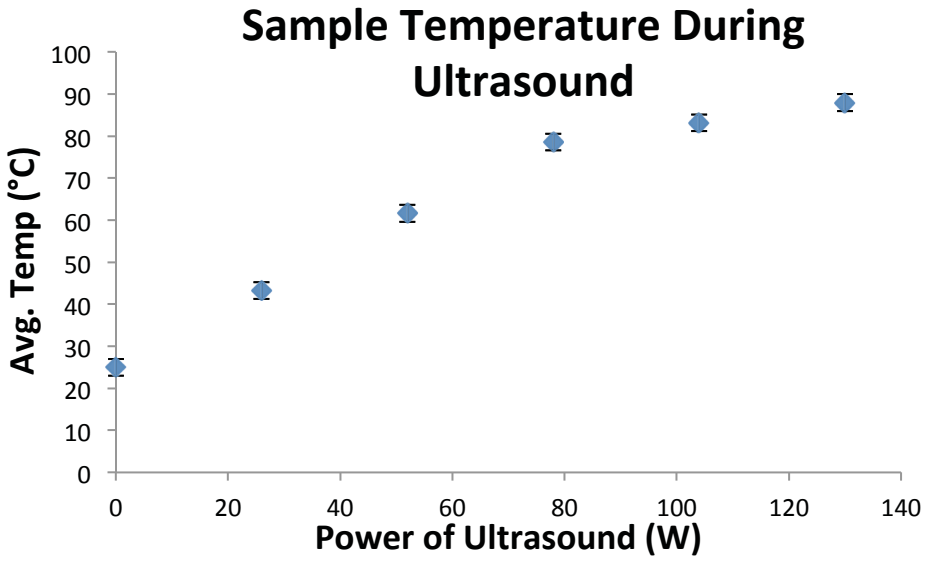

Figure 2.14. Final temperature of deionized water sample after inversion recovery experiment at varied ultrasound powers. Sample temperature was measured using a thermocouple at the end of the experiment (approximately 20 minutes). Experiment based on one trial with estimated error.

This temperature increase may be from the mechanical motions of the sonication probe and not bulk heating from cavitation implosions; however, the temperature increase could possibly be affecting the system. Figure 2.15 shows how viscosity and T_1 are related. Since viscosity and temperature are inversely related, sample heating could cause T_1 to decrease as

is shown in the region circled in purple in Figure 2.15.[8] The T_1 of water would tend to increase in the given temperature region[39] but some samples of future interest may have the reverse trend. Since temperature does vary T_1 it is important to eliminate this factor.

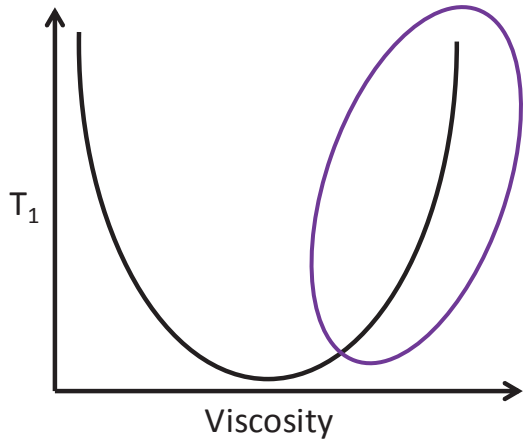

Figure 2.15. This illustration shows how T_1 and viscosity are related. In the region circled, T_1 decreases as temperature increases.

2.3.1 Instrumental Set-up

In an attempt to eliminate temperature effects during experiments, the sonication was pulsed as opposed to sonication during the entire experiment. Figure 2.16 shows the gated ultrasound. In the ideal case, illustration a, the sample only experiences sonication during the delay time of the inversion recovery experiment. During the delay time, τ, the spin-lattice relaxation is occurring. It is during this time that the paramagnetic radicals produced are interacting with the nuclear spins of the sample to increase relaxation, decreasing T_1. Illustration b in Figure 2.16 shows the actual case in the experimental set-up. A pulse is used to trigger the NMR on (1 ms) and the time it takes 2 ms to turn the sonicator on and off. Due to these facts, in order for the sonicator to be on during the entire delay time it was necessary to sonicate slightly before and slightly after the pulses of the inversion recovery experiment.

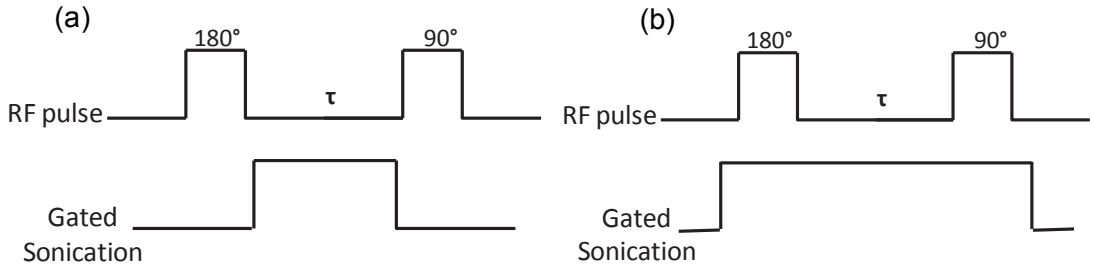

Figure 2.16. Illustration (a) shows the ideal case of gated sonication where ultrasound is only applied to the sample during the delay time of the inversion recovery experiment. Illustration (b) shows the actual experimental set-up due to experimental and instrument limitations

The VCX- 130 ultrasound generator and the TeachSpin NMR were interfaced using a National Instruments USB 6501 digital input/output device. An input/output device, or I/O device, is used to receive a signal from one system and then output a signal to another. The I/O device has a USB connection for computer connection. Connecting to a computer gives the device power but also allows control of the device using software. The I/O device also contains 24 digital input/output lines that use TTL (transistor-transistor logic). LabVIEW software was chosen to control the interfaced instruments due to its user-friendly operation.

A foot pedal can be used with the VCX-130 to turn the ultrasound on and off. This plug was utilized to connect the sonicator to the I/O device. A mono plug was purchased, the plug was inserted into the foot pedal connection of the sonicator and the other end of the cable was stripped and connected to the I/O device. A coaxial cable was connected to the NMR and the other end was stripped and connected to the I/O device. It was determined that bringing the sonicator (via the foot pedal switch) to zero volts, turned on the sonicator. Through the connection of the computer with LabVIEW software to the I/O device connected to the sonicator and NMR, a sequence was developed using the software to gate the sonication. The voltage to the sonicator was taken to “low”, zero volts, turning on the sonicator. A fixed delay was inserted

and then the NMR was triggered to give the inversion recovery pulse sequence. The software had a variable time delay that could be changed so that the time (sonicator was on) would match the delay time in the inversion recovery experiment. After this delay time, the voltage to the sonicator was brought "high", five volts, to turn the sonicator off.

To show that this method minimized sample temperature increase gated and non-gated scenarios were compared. When a sample of deionized water was sonicated for the duration of an inversion recovery experiment, without gated sonication, the average temperature reached from room temperature was 83.2 °C. For the same set of conditions but gated the sonication, the sample temperature reached 56.7 °C. Comparing the two indicates that by gating the sonication, the sample is not being heated as much.

2.3.2 Data: Measuring T_1 Using Gated Sonication

The experiments discussed in this section were conducted using the inversion recovery pulse sequence as described previously. The LabVIEW set-up was used to gate the sonication in efforts to minimize temperature increase of the sample. Figure 2.17 shows $T1/T_{1(0)}$ as a function of power of sonication applied.

(a)

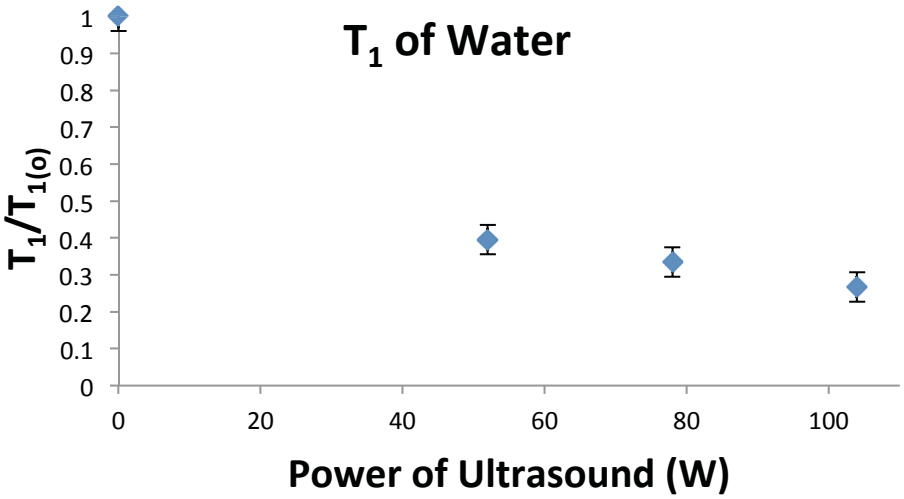

(b)

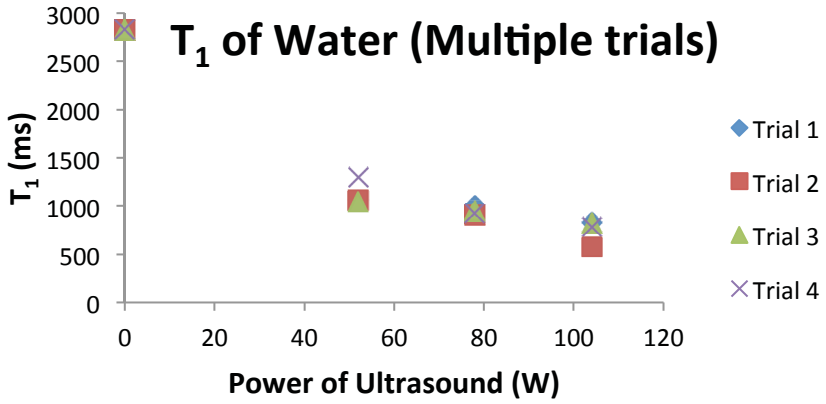

Figure 2.17. (a)This plot shows the decrease in T_1 in relation to ultrasound power. Decrease shown as $T_1/T_{1(0)}$, where T_1 is the measured T_1 during sonication and $T_{1(0)}$ is the T_1 measured when sample is not sonicated. Plot (b) shows the raw data of multiple trials averaged together to obtain plot (a)

The experimentally measured value of T_1 decreased with ultrasound power as it did when ultrasound was applied during the entire experiment. A comparison of the two experimental set-ups, gated and not gated ultrasound, is presented in the chart in Figure 2.18.

Ultrasound Power (W)	Not Gated $T_1/T_{1(0)}$	Gated $T_1/T_{1(0)}$
52	0.48	0.44
78	0.24	0.33
104	0.15	0.29

Figure 2.18. Comparison of gated and not gated sonication experiments. Sample used was deionized water. Decrease shown as $T_1/T_{1(0)}$, where T_1 is the measured T_1 during sonication and $T_{1(0)}$ is the T_1 measured when sample is not sonicated.

The data seems to show that temperature may not be an issue until a certain value of power of applied sonication is reached. When looking at the data in Figure 2.18, the decrease of T_1 is comparable for the two systems with 52 W of ultrasound power. The decrease of T_1 is significantly different when 104 W ultrasound is applied.

In previous experiments, the probe was positioned at the top of the sample, so it would not be in the coil and to minimize splashing. A study was conducted to compare the effect on T_1 when the probe position was changed. In the experiments, deionized water was used and sonicated with the probe near the bottom of the sample vial (within the coil) and with the probe at the top of the sample (not within the coil). The decrease in T_1 was greatest when the probe was at the top of the sample showing a 64% decrease in T_1 from the non-sonicated sample when sonicated with 78 W of power. When the probe was at the bottom of the sample vial, T_1 decreased by 33% from the non-sonicated sample when sonicated at 78 W of power.

With the help of Dr. Mark Lingwood, the coil height within the magnet of the TeachSpin NMR was measured and found to be 12 mm. In order to insure that the entire sample was being irradiated by the RF signal creating the 90° and 180° pulses, the sample size was decreased to 10 mm sample height in the vial. In previous experiments, the sample vial was full (30 mm sample height). Two experiments were conducted on deionized water: one with a 10 mm sample and the probe in the middle of the sample and another with a 30 mm sample and the probe at the top of the sample. For the 10 mm sample, a minimal decrease was seen in T_1 and in the 30 mm sample, there was a significant decrease. Only a 6% decrease in T_1 was observed for the 10 mm sample compared to a 79% decrease observed for the 30 mm sample. When looking at the raw date for the inversion recovery experiment, the signal for the for the 10 mm sample undergoing sonication was decreased from the signal when no ultrasound was applied. The zero-crossing, signature point indicating T_1, remains the same, only the maximum amplitude of the signal is decreased. For the 30 mm sample, the signal is decreased during sonication, but the zero-crossing also occurs at a shorter delay time, indicating a decrease in T_1. This may indicating that with a small sample volume, the sample is being “pushed” from the coil region where is detectable due to such a high power sonication being applied to a small volume.

2.3.3 Summary

In summary of section 2.3, the data shows that using the gated ultrasound system does appear to decrease the heating of the sample over the duration of the experiment. When sonicating the sample during the delay time of the inversion recovery pulse sequence, there is a trend between ultrasound power and decrease in T_1; as was seen with the non-gated system. Comparison of the gated and non-gated data shows that the decrease is T_1 is similar when lower sonication power is applied but at higher powers, the variance is larger between the two systems. Since the temperature increases with greater power of ultrasound, perhaps only at the higher temperatures T_1 is affected by temperature.

Sample volume and ultrasound probe position were also explored using the gated system. A greater decrease in T_1 was seen when the sample vial was full, containing 30 mm of deionized water, and the probe was positioned at the top of the sample, not in the coil. Upon visual inspection of the sonication of the 10 mm sample, it was seen that the sample was dramatically splashed out of the coil even at low powers of sonication. The sample contained vigorous bubbles and the sample was forced up the sides of the vial. When the sample vial contained a 30 mm sample, with the probe at the top of the sample, there were visual bubbles but no forced displacement of the sample out of the coil area. Perhaps the vigorous bubbling of the smaller sample is forming a barrier bubble around the probe tip so that the sample is not adequately sonicated in order to form free radicals.

2.4 Sample Mixing Effects

When sonicating a sample within the NMR tube used for the TeachSpin, it is readily apparent that the sample is being vigorously mixed due to the rapid movement of the bubbles being formed by the sonicator tip. Previous experiments indicated that when sonicating a sample that is completely contained within the NMR coil (no sample outside of coil region), there is no decrease in T_1. However, when the sample volume exceeds the volume of the coil (by a

factor of ~3), a decrease in T_1 is observed. These observations indicate that mixing may play a role in the observed decrease of T_1 and in addition to formation of paramagnetic free radicals. This may also explain the error in reproducing the sonication experiments as the amount of mixing may vary. As the sample is being sonicated, spins within the coil are being mixed with spins outside of the coil.

2.4.1 Formation of Free Radicals

Are free radicals being produced while sonicating? This is the first question that was attempted to be answered experimentally. As discussed previously, spin traps can be used to indicate radical production.[24, 27] Free radicals are very reactive and not easily monitored directly, and after sonication is stopped the radicals quickly dissipate. By experimentally observing the products formed from the reaction of the produced free radicals with an added reagent, we can indicate the concentration of free radicals produced.

Chakinala *et al.* investigated the efficiency of sonication with varied parameters by sonicating aqueous solutions of salicylic acid and observing the concentration of major products of 2,5-dihydroxybenzoic acid (2,5-DHB) and 2,3-dihydroxybenzoic acid (2,3-DHB) through HPLC.[27] Figure 2.19 shows the products of salicylic acid solutions sonicated, and the concentration of these products over time of sonication.

(a) Salicylic acid 2,3-DHB 2,5-DHB

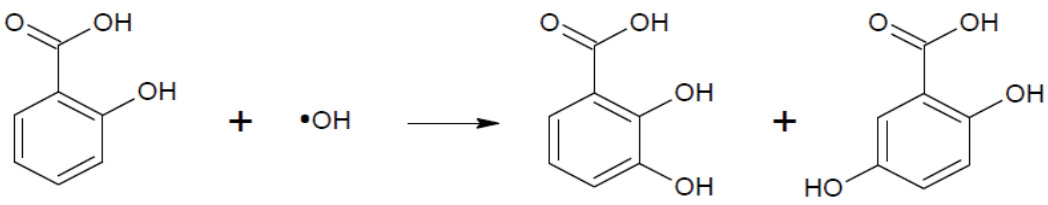

(b)

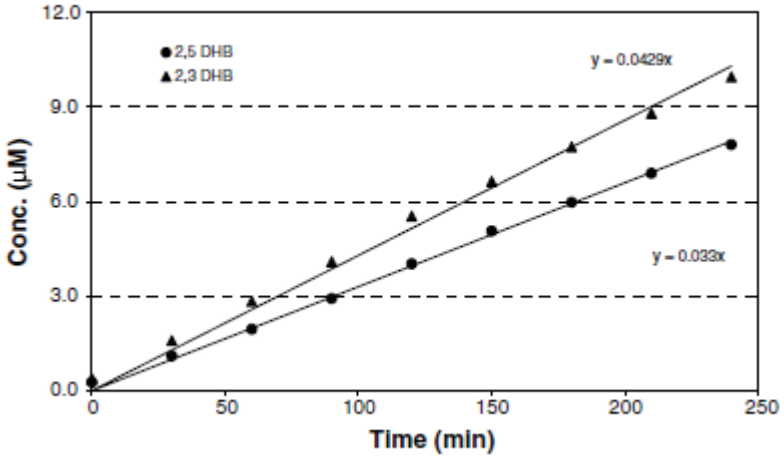

Figure 2.19. The sonication products of salicylic acid solution are shown in (a), while (b) shows the concentration of these products as a function of sonication time. Figure (b) was reproduced from Reference 27.

A solution of 0.01 M salicylic acid was prepared and the ^{1}H-NMR was collected at 600 MHz. The sample was placed in the TeachSpin NMR vial (full vial) and sonicated for 10 seconds with 104 W of ultrasound power using the 2 mm microprobe tip. The probe was positioned at the top of the sample to replicate sonication experiments. These conditions were chosen because they replicate the sonication length and intensity during a T_1 measurement. After sonication, the sample was transferred to a 5 mm NMR tube and the ^{1}H-NMR spectrum was collected at 600 mHz. Figure 2.20 shows the ^{1}H-NMR spectra. If dihydroxybenzoic acid was being formed due to combination with $^{\cdot}$OH radicals, a decrease would have been seen in peaks 3 and 5 as the hydrogens were replaced with hydroxyl groups. As can be seen in Figure 2.20, there is no difference seen in the two spectra, perhaps indicating that hydroxyl free radicals were not formed. The peaks were integrated and no difference was found between the two samples. When using the linear regression equations given in Figure 2.19(b), and the 1:1 ratio between dihydroxybenzoic acid and OH radicals, , it was calculated that during sonication of 10 seconds, the concentration of hydroxyl free radicals should be 0.077 µM with a starting

concentration of salicylic acid of 0.5 mM. Though the sonication amplitudes, sample volumes, and salicylic concentrations were different, it is possible to conclude that not enough products were formed to be detected using ^{1}H-NMR.

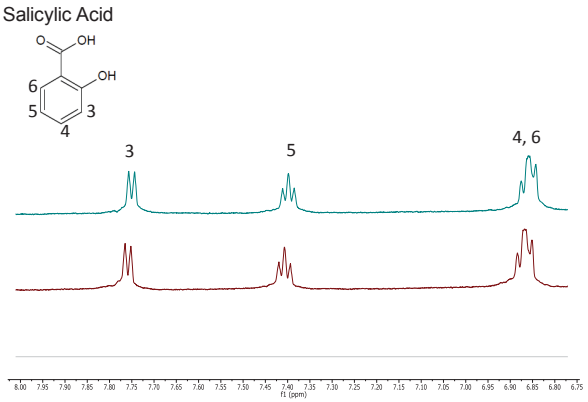

Figure 2.20. ^{1}H-NMR of salicylic acid solutions. The non-sonicated salicylic acid is shown in blue and the sonicated salicylic acid is shown in red. There is no difference in the two spectra.

2.4.2 Mixing of Sample

Since detecting products formed from the sonication of water through ^{1}H-NMR proved to be difficult, the decrease in T_1 was measured while physically mixing the sample. The T_1 of water was measured on the TeachSpin NMR using the inversion recovery method. Then, the T_1 of a sample was measured while bubbling air into the sample to simulate the mixing that occurs during sonication. The sample vial was half full during bubbling to minimize splashing. Tubing was connected to an air valve on one end and a glass pipet on the other which was inserted into the sample. The gas flow was adjusted so that, visually, the amount of mixing was similar to that involved in sample sonication.

While bubbling the sample the T_1 was measured to be 1.5 seconds as an average of two trials with a %RSD of 2. This gives a $T_1/T_{1(0)}$ of 0.68 due to mixing. The bubbling rate was

decreased slightly and $T_1/T_{1(0)}$ was found to be 0.73 T_1 with a %RSD of 0 between two trials. This indicates that more vigorous mixing leads to more error in the measurement.

To further investigate the error in maximum amplitude readings while bubbling, ten consecutive readings (maximum amplitude) were taken at two different delay times of both water while bubbling and water not bubbled. The error at a delay time of 350 ms was found to be 9% RSD for the sample without bubbling and 1% RSD for the sample while bubbling. With a delay time of 1250 ms, the error in the bubbling sample was found to be 38% RSD and 23% RSD for the sample that was not subjected to bubbling. This shows that error is greater when the sample is being mixed and also that the error is higher near the zero crossing point in the inversion recovery experiment.

A comparison of the T_1 curves for the bubbled water and the non-bubbled water is shown in Figure 2.21. Both follow an exponential T_1 curve but the characteristic time constant of the curves are different leading to different T_1 values. At low delay times, the curves seem similar and again at higher delay times it appears that the curves will level out around the same maximum amplitude. Due to instrument constraints with the TeachSpin NMR, the delay time cannot be increased beyond 10 seconds.

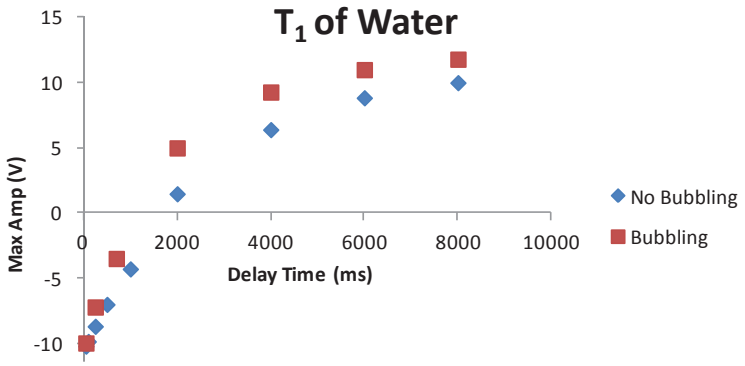

Figure 2.21. Plot showing the shape of the inversion recovery T_1 curves of a deionized sample where T_1 was measured while bubbling (mixing) compared to a deionized sample that was not bubbled (non-mixed) during the experiment. Example inversion recovery plots from one trial.

Upon further investigation, the decrease in T_1 due to sample mixing can be explained. In the sonication experiments described previously, it was found that a decrease in T_1 was only observed when the sample vial was full. With a full sample vial, 2/3 of the sample is outside of the coil region while only 1/3 of the sample is within the coil experiencing the RF pulses and giving rise to the observed signal. In the following is a discussion of how the signal would be affected at four representative different points along the T_1 curve due to mixing; these ideas are also visualized in Figures 2.22 - 2.25. Imagine splitting the sample vial into thirds, where only the middle third is the portion within the coil which will experience the RF pulses as well as emit a detectable signal. The arrows in Figures 2.22 - 2.25 represent individual spins with the purple arrows being those outside of the coil when the initial 180° pulse is applied and the red arrows representing the spins within the coil when the 180° pulse is applied. Mixing is considered to take place during the delay time between the 180° pulse and the 90° pulse.

The first point to be considered is the amplitude of the signal taken after a very short delay time, before the zero crossing, where mixing can essentially be ignored. Figure 2.22 shows a comparison of a sample that is mixed compared to a sample that is not. It can be seen that since mixing can be ignored due to the short time, the signals in the mixed and unmixed cases are the same at very short delay times.

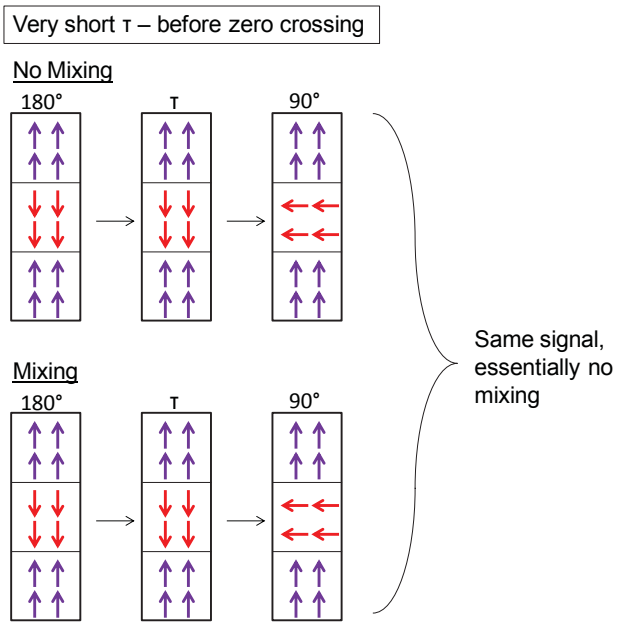

Figure 2.22. Comparison of a mixed sample and an unmixed sample at a very short delay time before the zero crossing. The middle section (vertically) is the part of the sample detected by the NMR coil.

The next point depicted in Figure 2.23 is a comparison between mixing and not mixing at short delay time still before the zero crossing. In this case, mixing is considered and during the delay time some spins that originally did not see the 180° pulse are mixed into the coil region while some of the spins that did see the 180° pulse are no longer within the coil region. Only the spins that experienced the 180° pulse are relaxing back to equilibrium. When comparing the signal obtained after the 90° pulse from the two scenarios, it can be seen that the signal from the sample experiencing mixing would be in the opposite phase of the signal from the unmixed sample. This would change the apparent zero crossing as well as lead to less observed signal when mixing.

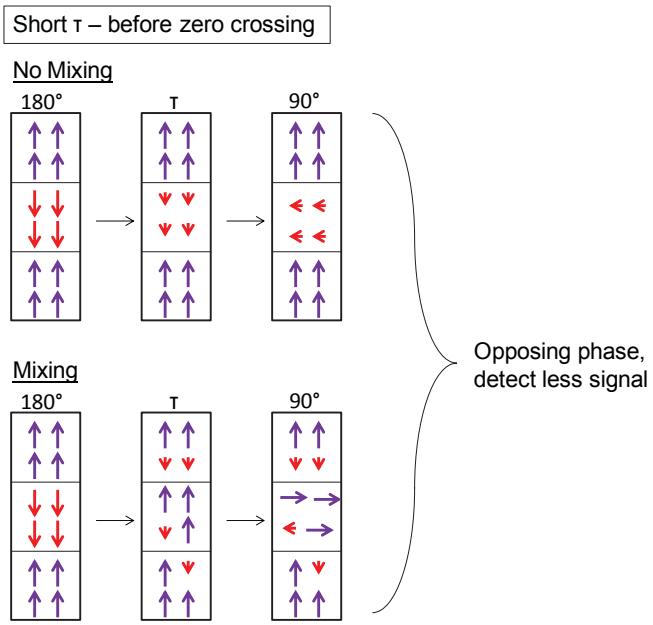

Figure 2.23. Comparison of a mixed sample and a non-mixed sample at a short delay time before the zero crossing. The shorter arrows represent spins with a lower signal during the relaxation process from inversion to equilibrium.

Figure 2.24 compares the signal obtained from mixing to that of not mixing after the zero crossing of the inversion recovery experiment, at a moderate delay time. At this point along the T_1 curve, the signals from the mixed sample and the unmixed sample would be in the same phase when the 90° pulse is applied leading to an increase in the signal from the sample undergoing mixing.

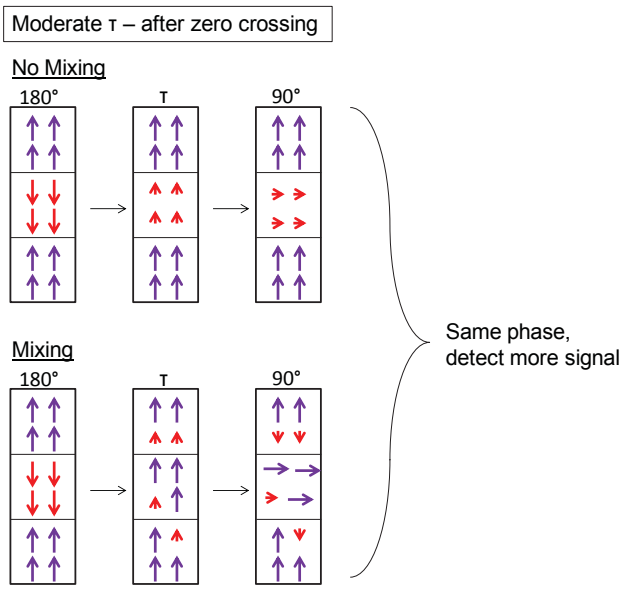

Figure 2.24. Comparison of a mixed sample and a non-mixed sample at a moderate delay time after the zero crossing.

The final point to investigate is at a very long delay time. In this case the spins that have experienced the 180° pulse have fully relaxed back to their equilibrium state. This gives the same signal when mixing the sample as well as when the sample is not being mixed. Figure 2.25 shows the comparison of these two cases.

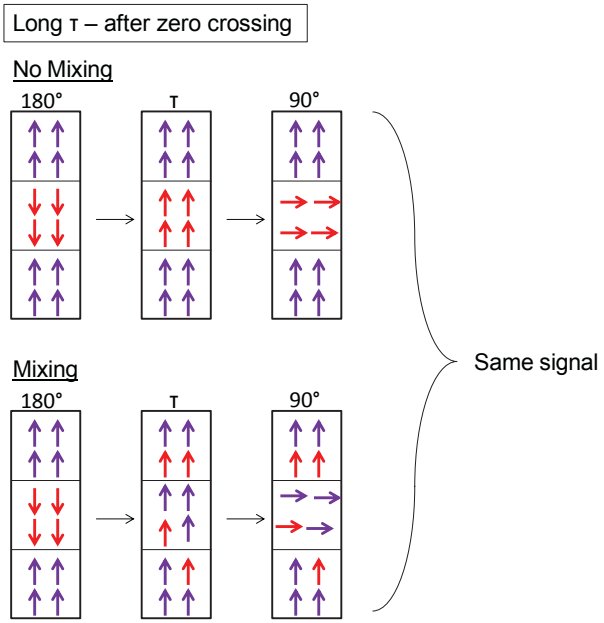

Figure 2.25. Comparison of a mixed sample and a non-mixed sample at a long delay time after the zero crossing.

To summarize, at very short delay times the signal from the two cases would be essentially the same. At short delay times, before the zero crossing, the signal would be decreased due to mixing. For moderate delay times after the zero crossing, the signal would be increased in the mixed sample. Finally, at long delay times, the signal would be the same for the mixed and the non-mixed samples. Figure 2.26 shows what the two scenarios would look like upon plotting an inversion recovery T_1 curve. It can be seen that the zero crossing of the sample being mixed is decreased from the zero crossing of the non-mixed sample which would give a decrease in T_1. The plot in Figure 2.26 is very similar to the plot in Figure 2.21 showing the experimental data of bubbling (mixing) and no bubbling (no mixing). This indicates that mixing does in fact decrease apparent T_1.

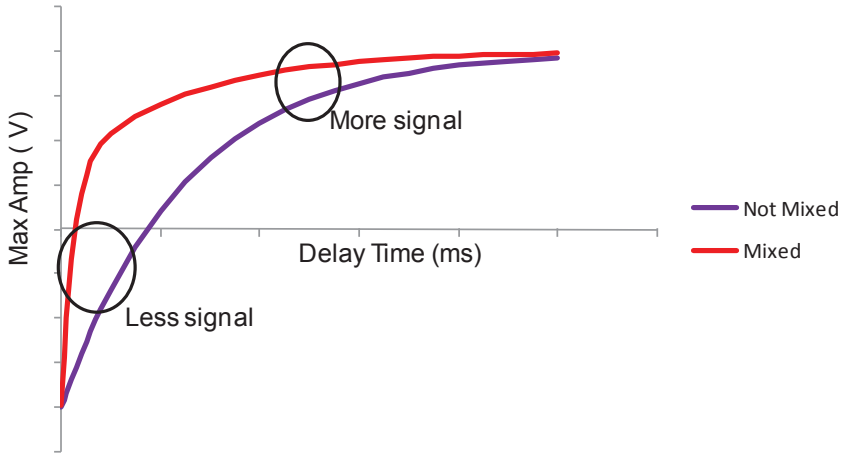

Figure 2.26. Comparison of the inversion recovery plots of a mixed sample and a non-mixed sample. In this scenario, homogeneous mixing occurs around 2 seconds and the apparent (observed) decrease in T_1 is 81%.

2.4.3 Simulated T_1 Artifacts Due to Mixing

Now that it is established that mixing a sample larger than the RF coil does show an apparent decrease T_1, it is important to think about how the mixing rate influences that decrease. The mixing rate can be thought of the amount mixed per unit time. As the process of mixing begins, it is assumed that the mixing occurs at an increased rate. When mixing is complete, a homogeneous mixture has been achieved, and the rate will level off. Figure 2.27 shows a plot of the mixing rate with the assumption that mixing is an exponential process where it takes some time for mixing to reach a state of homogeneity in the mixture but once it reaches homogeneity, it remains homogeneous. A mixing extent of zero indicates that no mixing has occurred while a mixing extent of one indicates that the mixture is completely mixed and a homogeneous mixture has been achieved.

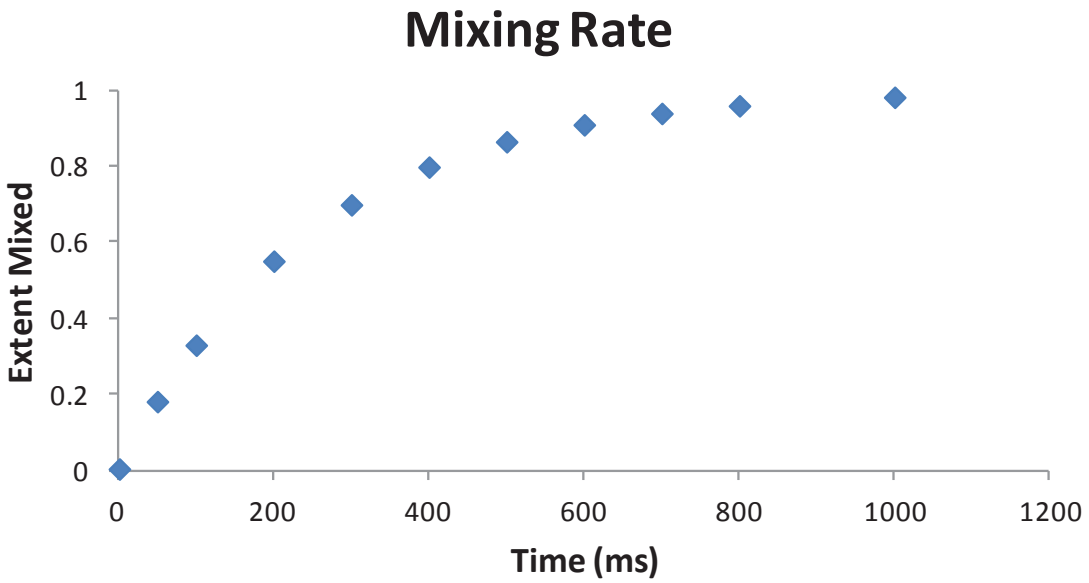

Figure 2.27. Process of mixing showing an exponential increase in extent mixed over time.

It is necessary to consider mixing rate when thinking about how mixing can decrease T_1 when measured by inversion recovery. Below the zero crossing, the more the sample is mixed, the lower the signal is compared to the non-mixed sample. Above the zero crossing, the increase in signal is proportional to the amount mixed. This leads to the conclusion that the more the sample is mixed, or the faster that mixing occurs, the greater the decrease in T_1. Also, since the mixing extent would increase through the experiment, the inversion recovery experiment will produce bi-exponential data, where one exponential is due to T_1 decay and the other is due to the progress of mixing. This arises from the fact that the extent mixed is increasing until the sample reaches homogeneity. Figure 2.28 shows the inversion recovery curves for a sample of deionized sonicated with 104 W of power of sonication and a sample of deionized being mixed through bubbling. It can be seen by comparing the two plots that the sample being sonicated appears to have two components while the bubbling sample appears to have a single exponential component. An attempt was made to fit the sonicated data with a two

component exponential in order to extract two different exponential time constants. The number obtained was not realistic as it gave a T_1 value of nearly 9 seconds. Even though fitting with a biexponential was unsuccessful, a difference between to the two plots can be observed. Perhaps this is due to the fact that for the bubbling sample, mixing is the only factor decreasing T_1 but for the sonicated sample T_1 is being decreased by mixing (where the mixture eventually becomes homogeneous) and paramagnetic hydroxyl radicals.

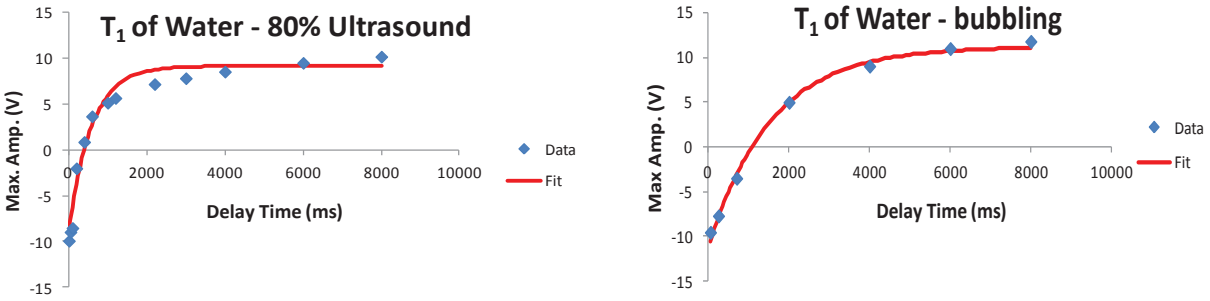

Figure 2.28. Comparison of the inversion recovery plots of deionized water being sonicated and a sample being mixed through bubbling. Example plots from one trial.

To simulate mixing's effect on T_1, an equation was developed to describe the overall detected magnetization of the sample:

$$M_z = (\frac{2}{3} I \times M_{eq_1}) + ((\left(1 - \frac{2}{3} I\right) \times M_{eq_2}) \quad (2.1)$$

M_{eq1} is the magnetization of the spins that were not originally in the coil to receive the 180° pulse and is the value of the maximum equilibrium magnetization as these spins are not undergoing relaxation. M_{eq2} represents the magnetization of the spins that started in the coil when the 180° pulse was applied and these spins are relaxing back to the original equilibrium magnetization. The factor of 2/3 was used because 2/3 of the sample is outside the coil region while 1/3 is

within the coil. I is defined as the extent mixed and I = 0 indicates that the sample is non-mixed and all the signal comes from the spins that experienced the 180° pulse. A value of one for I indicates that the sample is entirely mixed and 2/3 of the signal comes from spins that were not in the coil during the 180° pulse and 1/3 of the signal comes from spins that were originally within the coil region. More specifically, I can be described by

$$I = 1 - e^{-\tau K_{mix}} \tag{2.2}$$

Here, τ is the delay time used in the inversion recovery experiment and K_{mix} is 1 over the mixing time; the mixing rate. K_{mix} is a variable parameter used to adjust the mixing rate, which is how quickly the sample becomes homogeneous.

By using Equations 2.1 and 2.2, data can be simulated with varied mixing rates. That data can then be fit to the inversion recovery equation to obtain a T_1 that can be compared to the T_1 of sample not undergoing mixing in order to see how much T_1 will decrease when mixing. Figure 2.29 gives data obtained from simulation and shows the decrease in T_1 while mixing. In one case, homogeneous mixing occurs at a mixing time of nearly 10 second. This gives an apparent decrease in T_1 where $T_1/T_{1(0)}$ is 0.67 upon mixing. In the second case, homogeneous mixing occurs much faster at approximately 500 ms. This gives an apparent decrease in T_1 where $T_1/T_{1(0)}$ is 0.09. While there were several assumptions involved in this simulation, such as modeling mixing as an exponential process and arbitrarily setting the mixing time, this data obtained from simulation does clearly illustrate the effect of mixing on the measured T_1 value.

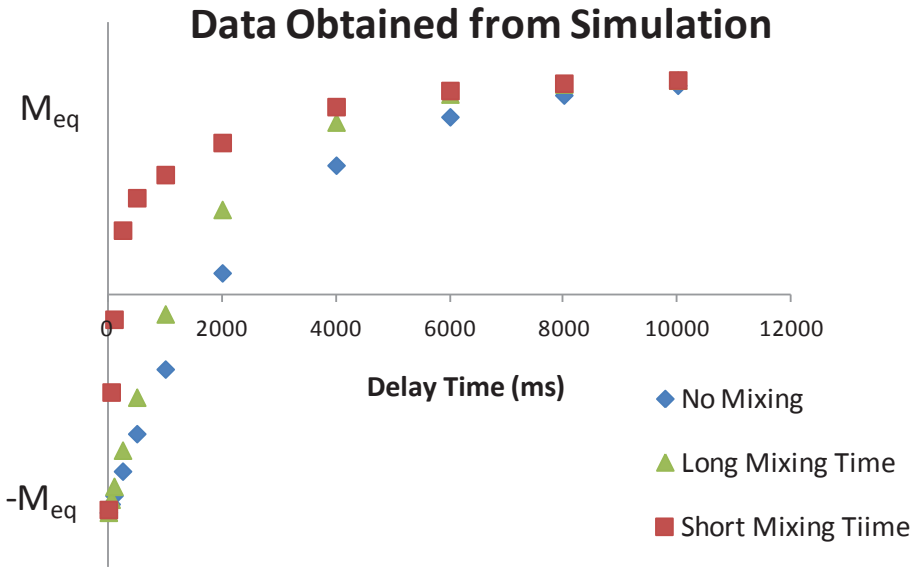

Figure 2.29. Data obtained by simulation based on Equation 2.1 showing how mixing leads to an apparent decreases T_1 at long mixing times and short mixing times. In both cases the decrease is compared to an original T_1 of 2.5 seconds and the equilibrium magnetization is 4 V.

Mixing effects can be considered when accounting for the data showing that higher sonication amplitude gives a greater observed decrease in T_1 (section 2.2.2). At higher sonication powers, the sample is being mixed more vigorously leading to homogeneity being reached sooner giving a greater observed decrease in T_1. Figure 2.30 shows the inversion recovery plots of data collected while sonicating deionized water at varied powers. This plot is similar to the plot given in Figure 2.29 correlating mixing rate and apparent decrease in T_1.

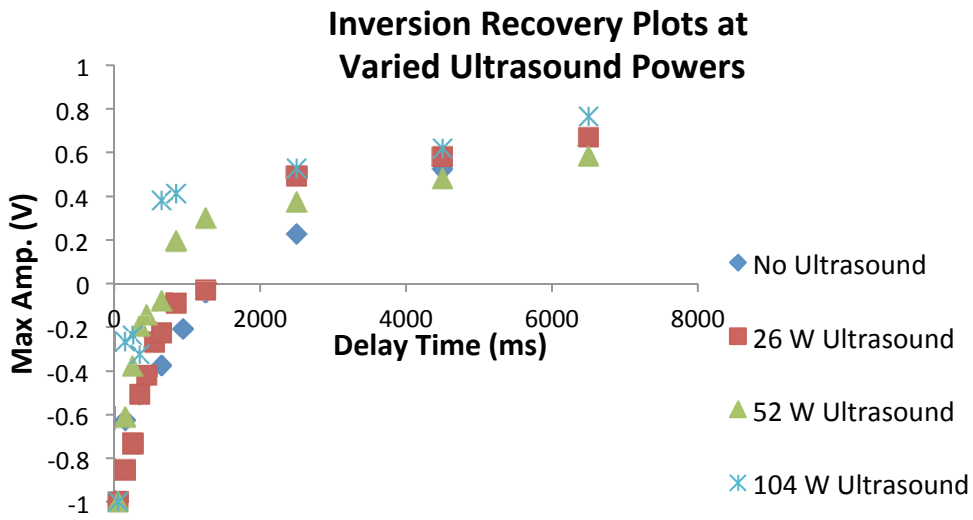

Figure 2.30. Inversion recovery plots of deionized water at different ultrasound powers showing that perhaps increased amplitudes indicates homogeneity being reached sooner due to mixing. Example plots from one trial.

To further investigate the apparent decrease and its dependence on free radical production, mixing, or both, the inversion recovery plot of deionized water sonicated at 104 W of power was fit with both the T_1 equation (equation 1.3) and the mixing equation (equation 2.1). This is shown in figure 2.31. Equation 2.1 gives a better fit than equation 1.3; however only one variable, the mixing time, was varied to get the fit for the mixing case. With this fit, homogenous mixing must occur within 1×10^{-12} ms. This is almost instantaneous mixing which is perhaps possible but is still an unknown variable.

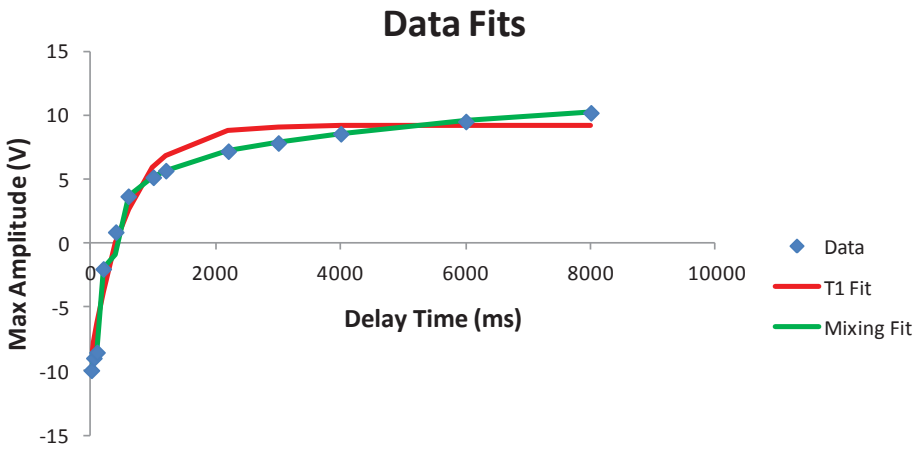

Figure 2.31. Inversion recovery data from 80% ultrasound of deionized water fit with T_1 equation and mixing equation.

2.4.4 Summary

To conclude the discussion of mixing effects, it was determined that mixing does lead to an apparent decrease T_1 when the entire sample is not contained within the coil region of the spectrometer. A fist attempt was made to determine if radicals were being formed during the sonication of the sample. This proved to be difficult and yielded no promising results. The next step was to investigate how mixing influenced the apparent T_1. Through a thought experiment, it was shown that at short delay times mixing leads to a decrease in signal and at long delay times there is an increase is signal. This leads to an overall apparent decrease in T_1 when compared to a sample that is not being mixed. The extent to which T_1 is decreased appears to be dependent on the mixing rate. If the sample reaches homogeneity more quickly, the observed decrease in T_1 is greater.

The data and simulations show that the apparent T_1 is decreased by sample mixing and perhaps the decrease seen while sonicating the sample was from the mixing incurred as well as to the actual formation of paramagnetic hydroxyl radicals. This leads to thinking about viscosity of different samples as viscosity would play a role in mixing. The T_1 of water, hexane, and

methanol was measured while sonication at 104 W of sonication power using the gated set-up and compared to the T_1 while not sonicating. The decrease seen in all three samples was similar with a $T_1/T_{1(0)}$ of 0.21 seen in water, 0.22 in hexane, and 0.20 seen in methanol. The viscosities at 25°C of water, hexane, and methanol are 0.890 mPa s, 0.300 mPa s, and 0.544 mPa s respectively.[40] With water being much more viscous than hexane, if mixing were the only cause for T_1 decrease, it would be reasonable to assume that the decrease in hexane's T_1 would be much greater than observed in water. Also, in section 2.2.1, data is presented showing that as concentration of radical-producing species increases, the observed decrease in T_1 is enhanced upon sonication. This does not support sample mixing being the only influence in T_1 decrease because each sample was sonicated with the same sonication amplitude.

Chapter 3
Conclusion

Using ultrasound to produce free radicals holds promise for uses in a wide array of analytical techniques. Free radicals could possibly be used as contrast agents, in polymer reactions, and in dynamic nuclear polarization. By sonicating a sample *in situ*, contrast might be obtained in MRI without having the patient ingest paramagnetic species, polymer reactions involving free radicals might be controlled and monitored, and the unpaired electron might be used for signal enhancement in dynamic nuclear polarization. Understanding how free radicals are formed and the experimental parameters that can be optimized to increase sonochemical yield, can help in the development of this technique and its applications.

In the literature cited, the processes of cavitation and radical formation were observed by either analytical analysis of products formed from radicals, by spin-trapping, or by EPR of long-lived radicals. In most cases the radicals are transient and some may be lost during analysis through recombination. With our research, we propose a new method to investigate sonochemistry by *in situ* sonication. This could potentially lead to a better understanding of cavitation and how to get maximum cavitation bubble production, and thus, maximum radical production.

The literature discussed in this document has given insight into how to increase radical production by optimizing parameters, but it is also important to understand why concentration plays a role. Because the decrease in T_1 depends on the water molecules' interaction with the paramagnetic radicals, at higher concentrations each radical interacts with fewer water molecules, thus leading to more water molecules being affected and relaxation rate increasing. The diffusion of the water molecules must also be considered. In higher concentrations, the diffusion length of water molecules in one Larmor Precession is larger than the sphere of water

influenced by one radical. Again, this results in more water molecules being influenced by the paramagnetic radical.

The experiments conducted for this document were done using a TeachSpin NMR with a 0.36 T permanent magnet. The TeachSpin was used to find the T_1 of the samples using the inversion recovery pulse sequence. The sonication was produced using a VCX-130 ultrasound generator, which was used to sonicate the sample within the TeachSpin magnet using both 2 mm and 3 mm probe tips.

Concentration and sonication power were the first parameters investigated. It was found that in both cases, hydrogen peroxide and benzoyl peroxide, the decrease in T_1 observed was increased when the concentration of the sample was increased. Also, using higher sonication powers maximized the decrease seen in T_1. These finding are consistent with the literature in that an increase in the concentration of radical-producing species, as well as the sonication amplitude used, produces more free radicals. An increase in free radical production would lead to a greater decrease in the measured T_1 value.

While conducting experiments using *in situ* sonication, it was found that the temperature of the sample increased throughout the experiment; most likely due to mechanical heat from the sonication probe. In efforts to eliminate this temperature increase, which could be affecting the T_1, sonication was gated so that the sample only underwent sonication during the delay times of the inversion recovery experiment. The TeachSpin and VCX-130 ultrasound generator were interfaced using an input/output device and LabVIEW software for control. Gated sonication did reduce the overall temperature gain during the experiment. Higher sonication powers lead to a greater increase in the temperature in deionized samples when the sonication was continuous. When comparing the gated to the non-gated scenarios at 104 W of sonication power, the difference in T_1 values was 48% in a deionized sample; higher than the difference observed at lower sonication powers. The decrease in T_1 at 104 W of sonication power was higher for the

non-gated system. Perhaps this indicates that the temperature effect on T_1 is only an issue at higher sonication powers, which is where the maximum decrease in T_1 is observed.

During the gated sonication experiments, it was also discovered that a decrease in T_1 was only seen when the sample vial was full and the probe was at the top of the sample. In this set-up, only one third of the sample is within the coil region. During sonication, the sample is rapidly mixed due to bubble formation and movement of the sample from the mechanical motion of the sonication probe. This leads to some spins experiencing the pulses and others not with the spins being mixed. Given these facts, the question remains: is mixing causing an observed decrease in T_1? The first attempt to answer this was to monitor the production of radicals to show that they were in fact being formed during sonication to cause the observed decrease in T_1. When a salicylic acid aqueous solution is sonicated, 2,5-DHB and 2,3-DHB are the major products where the hydroxyl radical is substituted onto the ring. ^{1}H-NMR (600 MHz) spectra were collected on salicylic acid samples as well as sonicated salicylic acid samples to see if there was a change. No change was observed, however this could be due to the very low concentration of sonication products formed.

The next step in investigating the mixing effect on T_1 was to mix the sample by bubbling air through it and measuring the T_1. A $T_1/T_{1(o)}$ of 0.66 was observed in the T_1 of deionized; however, it was lower than that seen during sonication. This data gives supporting evidence that mixing does decrease T_1. Also, thinking through what signal changes might occur during an inversion recovery experiment due to mixing, it can be hypothesized that mixing should lead to an apparent decrease T_1. The signal would be lower at short delay times and increased at higher delay times which would lead to an overall decrease in T_1. Data was obtained through simulation to show this effect. The factor that determines the extent to which the observed T_1 is decreased is the time it takes for mixing to reach homogeneity.

In conclusion, these data show that *in situ* sonication does decrease T_1 and has promise in the potential suggested applications. Through experiment, we learned that sonicating samples of higher concentrations and using higher sonication power, results in a greater decrease. The effects of temperature can be reduced by gating the sonication so that the sample is only sonicated during the delay time as opposed to during the entire experiment. Sample mixing during sonication does lead to an apparent decrease T_1 when the sample is not entirely contained within the region of the coil which would be an issue for the suggested applications as they rely on a production of free radicals. Though mixing does lead to an observed decrease T_1, it may not be fully responsible for the observed decreases seen in experimental data. The mixing rate, time it takes for homogeneous mixing to occur, would determine the extent to which T_1 is decreased. Since data have shown that the decrease in T_1 is enhanced by an increase in the concentration of radical producing species, it is very likely that *in situ* ultrasound-induced free radicals are leading to a decrease in T_1.

Chapter 4
Future Work

Since it was determined that mixing decreases the apparent T_1 and the goal of this research it to determine if the sonication produces free radicals that would decrease T_1, it is necessary to eliminate the mixing effect. Future work would include re-designing the system so that the entire sample stays within the coil region. This could include making a new, larger coil for the NMR to ensure that the sample is not "pushed" out of the coil region. With a smaller volume of sample, the sonication power vigorously mixes the sample to such a degree that the sample is moved from the coil region. In order to have a larger sample volume that could withstand the sonication power and keep the entire volume within the coil region, a larger coil (taller coil) would be needed. The power density for a 3 mL sample sonicated at 104 W is 35 W/cm^3. Since the sonication power applied is too much for the small volume samples used in the TeachSpin NMR, it would also be useful to decrease the power supplied to the sonication probe. This could be done by adding a resistor to the sonicator circuit.

Another time constant studied in NMR spectroscopy is T_2 relaxation; also called spin-spin relaxation, and would also be effect by the production of free radicals and mixing. This time constant is related to the de-phasing of spins in the transverse plane due to magnetic field inhomogeneity. The decay in the transverse (x-y plane) follows the exponential curve in Figure 4.1. The curve can be fit to Equation 4.1 where T_2 can be extracted.[34,6]

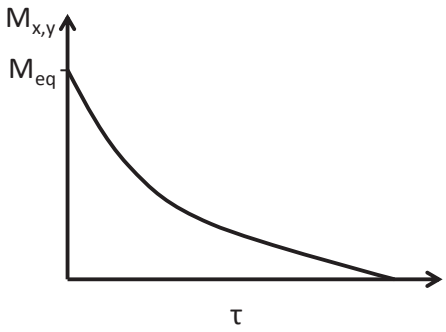

Figure 4.1. Exponential curve showing decay of magnetization in the transverse plane. M_{eq} is the original net magnetization and τ is time.

$$M_{x,y} = M_{eq} e^{\frac{-\tau}{T_2}} \tag{4.1}$$

Inhomogeneity in the magnetic field experienced by a given nuclei arises because each nucleus surrounding it is also acting as a magnet. This causes the nuclei to precess at varied frequencies which leads to de-phasing in the transverse plane and the net magnetic moment will go to zero.[6]

One simple two-pulse experiment used to measure T_2 is a spin echo experiment. The pulse sequence and vector model description can be seen in Figure 4.2. A 90° pulse is applied, which torques the net magnetic moment vector into the transverse plane. Some time, τ, is waited while the spins begin to de-phase as they are precessing at different frequencies, resulting in a decrease in the net magnetization. A 180° pulse is then applied which flips the spins in the transverse plans to rephase them. This leads to an echo signal at 2τ. By varying the time, τ, and measuring the intensity of the spin echo signal, a plot like Figure 4.2 can be constructed to extract T_2.[6, 34]

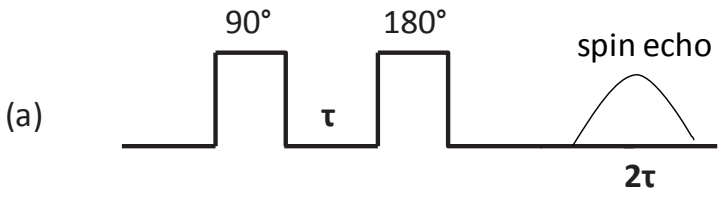

Figure 4.2. Part (a) is showing the Spin Echo pulse sequence and part (b) is showing the corresponding vector sequence.

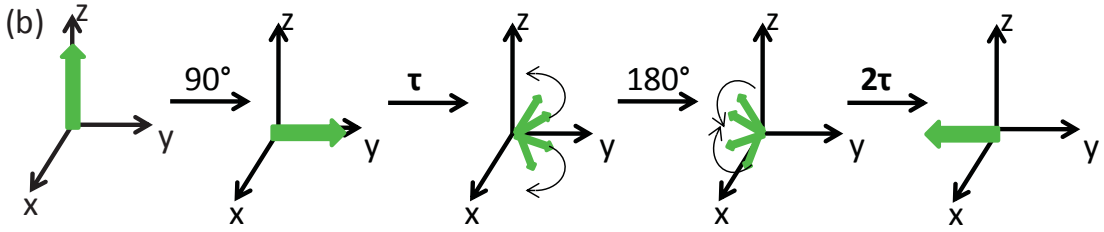

Future work proposed would include measuring the T_2 of deionized samples during sonication and during bubbling to simulate mixing. T_2 should also decrease when paramagnetic species are produced. Would T_2 also decrease with mixing? The answer is it most likely it will if the sample is mixed during the delay time and the 180° pulse that causes rephasing. The signal will decrease from the original signal observed after the 90° pulse, providing a decrease in the T_2 measured.

Chapter 5
Outreach Website: Play, Create, Discover

"*I always hear stories about how we can't find enough engineers, we can't find enough computer programmers… And that's why we're emphasizing math and science. That's why we're emphasizing teaching girls math and science. We've got to lift -- we've got to lift our game up when it comes to technology and math and science. That's, hopefully, one of the most important legacies that I can have as President of the United States."*
President Barack Obama
May 2011[41]

Getting young girls involved in science is on the agenda of many including our research group. In 2009, it was reported that only 24% of the science and engineering jobs in the United States were filled by women.[41] Some believe that there is a stigma associating science and math with males. This perception must be overcome by getting girls interested in science and math at an early age by fostering a desire to learn fundamentals through play and creativity. Our group has begun development of a website geared toward young girls which encourages them to investigate the world around them and ask questions that lead to discovery. The home page of the website, playcreatediscover.chem.vt.edu, is shown in Figure 5.1.

Figure 5.1. Home page of playcreatediscover.chem.vt.edu.

This website along with a kit and household items will encourage girls to explore scientific topics without being instructed. The kits include such things as goggles, beakers, lab notebook, glue, markers, rubber bands, magnets, iron filings, and more. Another feature of the website is a place for parents to see suggested activities which will lead the children to learn about things such as chromatography, magnetism, and polymers. The girls will be able to interact with other female scientists through a forum where they can ask questions about things they discover as they are playing. The home page also includes a fun fact and a short biography of a famous female scientist, both of which will be regularly changed. It is our hope that we can instill the love of science in young girls by providing a forum and the materials for them to play while learning.

References

1. Suslick, K. S.; Price, G. J., APPLICATIONS OF ULTRASOUND TO MATERIALS CHEMISTRY. *Annual Review of Materials Science* **1999**, *29* (1), 295-326.
2. Abragam, A.; Goldman, M., PRINCIPLES OF DYNAMIC NUCLEAR-POLARIZATION. *Reports on Progress in Physics* **1978**, *41* (3), 395-467.
3. Hickenboth, C. R.; Moore, J. S.; White, S. R.; Sottos, N. R.; Baudry, J.; Wilson, S. R., Biasing reaction pathways with mechanical force. *Nature* **2007**, *446* (7134), 423-427.
4. Kaupp, G., Mechanochemistry: the varied applications of mechanical bond-breaking. *CrystEngComm* **2009**, *11* (3), 388-403.
5. Saifutdinov, R. G.; Larina, L. I.; Vakul'skaya, T. I.; Voronkov, M. G., *Electron Paramagnetic Resonance in Biochemistry and Medicine*. Kluwer Academic/Plenum Publishers: New York, 2001.
6. Levitt, M. H., *Spin Dynamics, Basics of Nuclear Magnetic Resonance*. 2nd ed.; John Wiley & Sons Ltd: England, 2008.
7. Blümich, B.; SpringerLink Essential NMR for scientists and engineers. http://dx.doi.org/10.1007/b138660.
8. Roberts, J. D., *ABCs of FT-NMR*. University Science books: Sausalito, California, 2000.
9. Suslick, K. S., The Chemical Effects of Ultrasound. *Scientific American* **1989**, *260* (2), 80-86.
10. Mason, T. J.; Lorimer, J. P., *SONOCHEMISTRY: Theory, Application and Uses of Ultrasound in Chemistry*. Ellis Horwood Limited: England, 1988.
11. Riesz, P.; Kondo, T., Free radical formation induced by ultrasound and its biological implications. *Free Radical Biology and Medicine* **1992**, *13* (3), 247-270.
12. Okitsu, K.; Suzuki, T.; Takenaka, N.; Bandow, H.; Nishimura, R.; Maeda, Y., Acoustic Multibubble Cavitation in Water: A New Aspect of the Effect of a Rare Gas Atmosphere on Bubble Temperature and Its Relevance to Sonochemistry. *The Journal of Physical Chemistry B* **2006**, *110* (41), 20081-20084.
13. Thompson, L. H.; Doraiswamy, L. K., Sonochemistry: Science and Engineering. *Industrial & Engineering Chemistry Research* **1999**, *38* (4), 1215-1249.
14. Suslick, K. S.; Hammerton, D. A.; Cline, R. E., Sonochemical hot spot. *Journal of the American Chemical Society* **1986**, *108* (18), 5641-5642.
15. Makino, K.; Mossoba, M. M.; Riesz, P., Chemical effects of ultrasound on aqueous solutions. Evidence for hydroxyl and hydrogen free radicals (.cntdot.OH and .cntdot.H) by spin trapping. *Journal of the American Chemical Society* **1982**, *104* (12), 3537-3539.
16. Sostaric, J. Z.; Reiesz, P., Sonochemistry of Surfactants in Aqueous Solutions: An EPR Spin-Trapping Study. *J. Am. Chem. Soc.* **2001**, *123* (44), 11010-11019.
17. Misik, V., Nitric Oxide Fromation by Ultrasound in Aqueous Solutions. *J. Phys. Chem.* **1996**, *100* (45), 17986-17994.
18. Berkowski, K. L.; Potisek, S. L.; Hickenboth, C. R.; Moore, J. S., Ultrasound-Induced Site-Specific Cleavage of Azo-Functionalized Poly(ethylene glycol). *Macromolecules* **2005**, *38* (22), 8975-8978.
19. Wu, Z. L.; Lifka, J.; Ondruschka, B., Sonochemical reaction of selected cyclic C6Hx hydrocarbons in organic solvents. *Ultrasonics Sonochemistry* **2005**, *12* (1-2), 127-131.
20. Krishna, C. M.; Lion, Y.; Kondo, T.; Riesz, P., Thermal decomposition of methanol in the sonolysis of methanol-water mixtures. Spin-trapping evidence for isotope exchange reactions. *The Journal of Physical Chemistry* **1987**, *91* (23), 5847-5850.
21. Krishna, C. M.; Kondo, T.; Riesz, P., Sonochemistry of alcohol-water mixtures. Spin-trapping evidence for thermal decomposition and isotope-exchange reactions. *The Journal of Physical Chemistry* **1989**, *93* (13), 5166-5172.
22. Kondo, T.; Carmichael, A., SONOCHEMISTRY OF ACETONE AND ACETONITRILE IN AQUEOUS-SOLUTIONS - A SPIN-TRAPPING STUDY. *Free radical research communications* **1993**, *19*, S45-S53.

23. Misík, V.; Riesz, P., Recent applications of EPR and spin trapping to sonochemical studies of organic liquids and aqueous solutions. *Ultrasonics Sonochemistry* **1996**, *3* (3), S173-S186.
24. Kondo, T., Sonolysis of dimethyl sulfoxide-water mixtures: a spin-trapping study. *Journal of physical chemistry (1952)* **1993**, *97* (2), 522-527.
25. Petrier, C.; Jeunet, A.; Luche, J. L.; Reverdy, G., Unexpected frequency effects on the rate of oxidative processes induced by ultrasound. *Journal of the American Chemical Society* **1992**, *114* (8), 3148-3150.
26. Okitsu, K.; Ashokkumar, M.; Grieser, F., Sonochemical Synthesis of Gold Nanoparticles: Effects of Ultrasound Frequency. *The Journal of Physical Chemistry B* **2005**, *109* (44), 20673-20675.
27. Chakinala, A. G.; Gogate, P. R.; Burgess, A. E.; Bremner, D. H., Intensification of hydroxyl radical production in sonochemical reactors. *Ultrasonics Sonochemistry* **2007**, *14* (5), 509-514.
28. Entezari, M. H.; Kruus, P.; Otson, R., The effect of frequency on sonochemical reactions III: dissociation of carbon disulfide. *Ultrasonics Sonochemistry* **1997**, *4* (1), 49-54.
29. Carretta, P.; Lascialfari, A.; Laurent, S.; Elst, L. V.; Roch, A.; Muller, R. N., Structure, synthesis and characterization of contrast agents for magnetic resonance molecular imaging. In *NMR-MRI, μSR and Mössbauer Spectroscopies in Molecular Magnets*, Springer Milan: 2007; pp 71-87.
30. Bloembergen, N.; Purcell, E. M.; Pound, R. V., Relaxation Effects in Nuclear Magnetic Resonance Absorption. *Physical Review* **1948**, *73* (7), 679-712.
31. Carretta, P.; Lascialfari, A.; Corti, M., Basic concepts of Magnetic Resonance Imaging NMR-MRI, μSR and Mössbauer Spectroscopies in Molecular Magnets. Springer Milan: 2007; pp 89-110.
32. Russ, J. L. Studies of solution Paramagnetic-Substrate Nuclear and Electron Intermolecular Interactions. Virginia Tech, Blacksburg, 2006.
33. Tokuda, H., Physicochemical Properties and Structures of Room Temperature Ionic Liquids. 1. Variation of Anionic Species. *The journal of physical chemistry. B* **2004**, *108* (42), 16593-16600.
34. TeachSpin Manual. TeachSpin, Inc.: Buffalo, NY, 1997.
35. Alegria, A. E.; Lion, Y.; Kondo, T.; Riesz, P., Sonolysis of aqueous surfactant solutions: probing the interfacial region of cavitation bubbles by spin trapping. *The Journal of Physical Chemistry* **1989**, *93* (12), 4908-4913.
36. Granwehr, J.; Kockenberger, W., Multidimensional low-power pulse EPR under DNP conditions. *Appl. Magn. Reson.* **2008**, *34* (3-4), 355-378.
37. User's Guide; Autotune Series High Intensity Ultrasonic Processor 2004.
38. Masterson, W. L. a. H., C.N., *Chemistry Principles and Reactions*. 4th ed.; Harcourt College Publishers Orlando, 2001.
39. Voronovich, A. N.; Lilich, L. S.; Khripun, M. K., Study of the temperature dependence of spin-lattice relaxation in water. *Theoretical and Experimental Chemistry* **1972**, *5* (5), 501-502.
40. CRC handbook of chemistry and physics. *CRC handbook of chemistry and physics.* 1978.
41. Women and Girls in Science, Technology, Engineering, and Math (STEM) http://www.whitehouse.gov/sites/default/files/microsites/ostp/ostp-women-girls-stem november2011.pdf.